Radiative corrections for the MUSE experiment

Lin Li and Steffen Strauch
University of South Carolina

for the MUSE Collaboration

Supported in parts by the U.S. National Science Foundation: NSF PHY-2111050. The MUSE experiment is supported by the U.S. Department of Energy, the U.S. National Science Foundation, the Paul Scherrer Institute, and the US-Israel Binational Science Foundation.

ECT* Workshop “Radiative Corrections from medium to high-energy experiments”, Trento, July 18–22, 2022

MUon Scattering Experiment (MUSE) at PSI

Direct test of μp and ep interactions in a scattering experiment:

- higher precision than previously for μp,
- low-Q^2 region for sensitivity to the **proton charge radius**, Q^2 = 0.002 to 0.07 GeV^2,
- with μ^+, μ^- and e^+, e^- to study possible **2γ mechanisms**,
- with μp and ep to have direct **μ/e comparison**.

MUSE

$$e^- p \rightarrow e^- p$$
$$e^+ p \rightarrow e^+ p$$
$$\mu^- p \rightarrow \mu^- p$$
$$\mu^+ p \rightarrow \mu^+ p$$

The MUon Scattering Experiment at PSI (MUSE), MUSE Technical Design Report, arXiv:1709.09753 [physics.ins-det].

Projected MUSE proton charge-radius results

How different are the e/μ radii?
(truncation error largely cancels)
Sensitivity to differences in extracted e/μ radii:

$\sigma(r_e - r_\mu) \approx 0.005$ fm

What is the radius?
Absolute values of extracted e/μ radii
(assuming no +/- difference seen):

$\sigma(r_e), \sigma(r_\mu) \approx 0.008$ fm

Comparisons of **e to μ** or of **positive to negative** are insensitive to many of the systematics

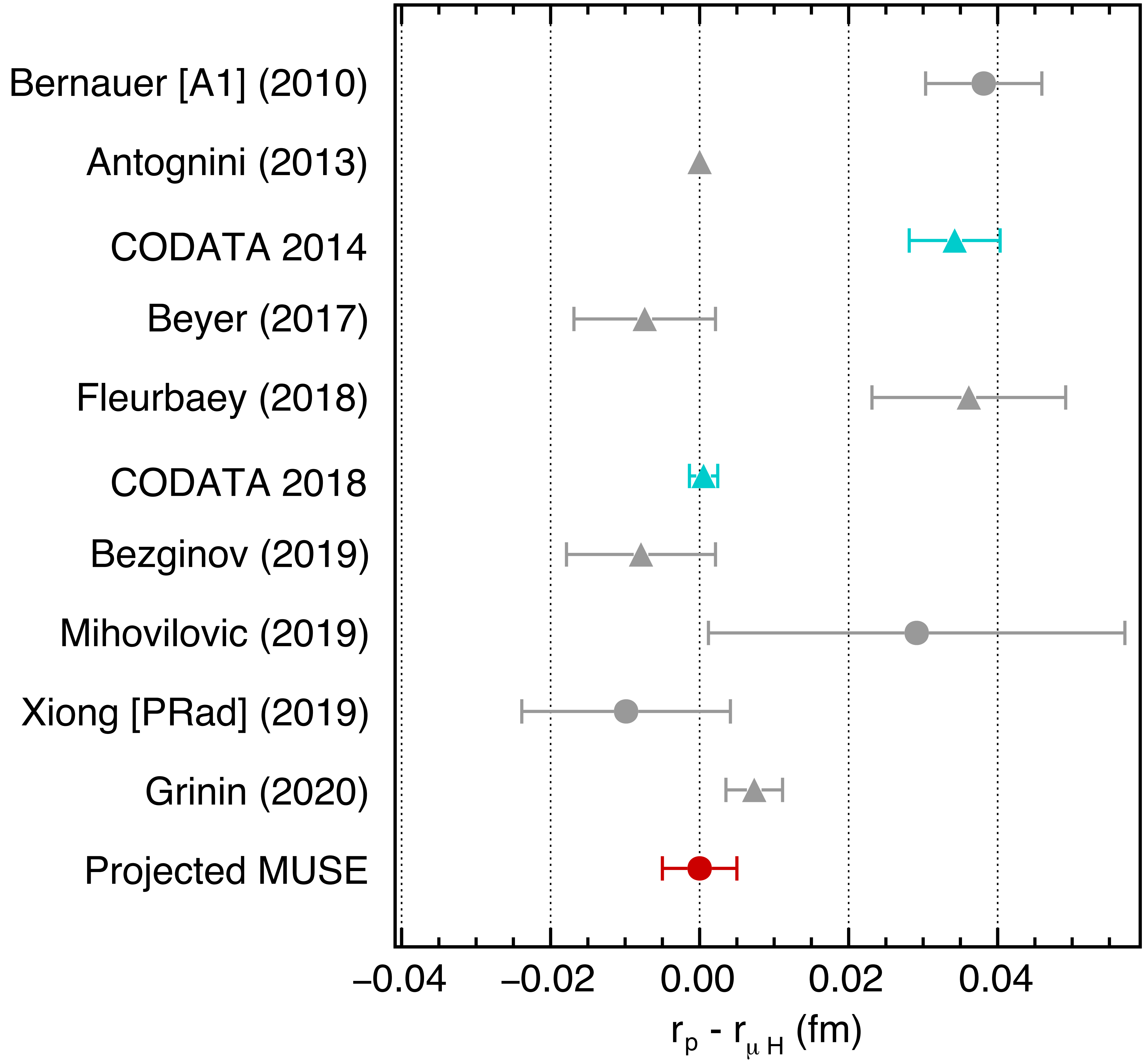

The MUon Scattering Experiment at PSI (MUSE), MUSE Technical Design Report, arXiv:1709.09753 [physics.ins-det].

Anticipated e and μ data for G_E from MUSE

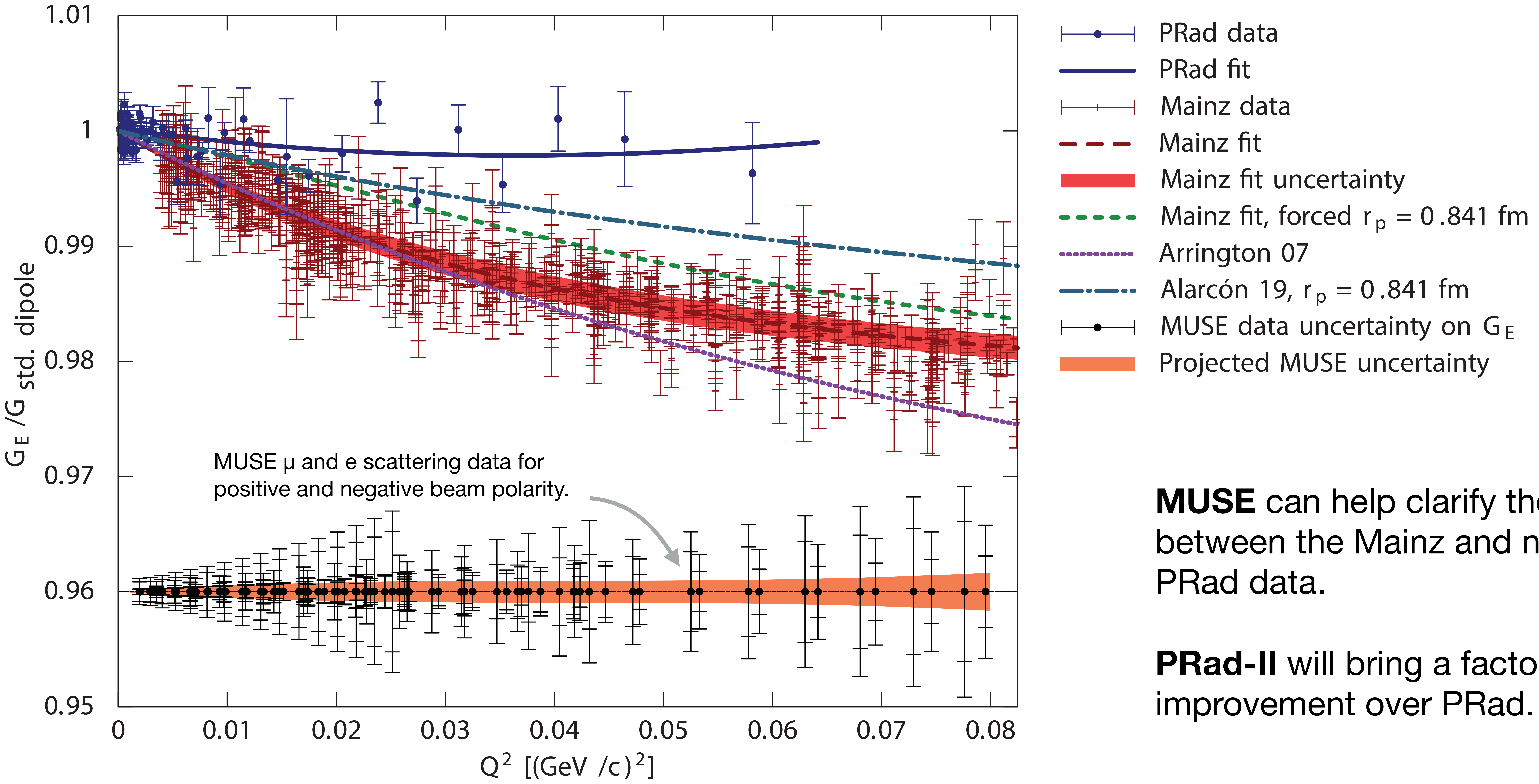

MUSE can help clarify the tension between the Mainz and new PRad data.

PRad-II will bring a factor of 4 improvement over PRad.

E. Cline, et al., SciPost Phys. Proc. 5, 023 (2021)

MUSE directly compares μp to ep cross sections

Projected relative statistical uncertainties in the ratio of μp to ep elastic **cross sections**.
Systematics ≈ 0.5%.

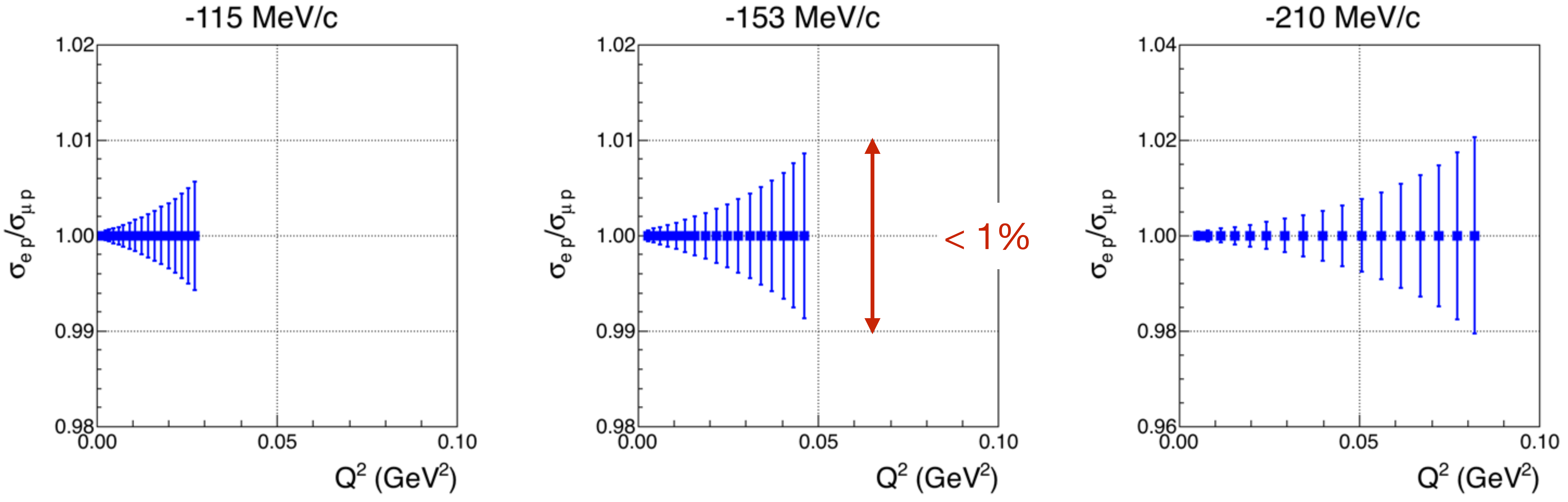

The relative statistical uncertainties in the **form factors** are half as large.

The MUon Scattering Experiment at PSI (MUSE), MUSE Technical Design Report, arXiv:1709.09753 [physics.ins-det].

MUSE allows to study two-photon exchange

Projected relative uncertainty in the ratio of μ^+p to μ^-p elastic cross sections. Systematics: 0.2% in the cross section ratio (0.1% in $\delta_{2\gamma}$).

The MUon Scattering Experiment at PSI (MUSE), MUSE Technical Design Report, arXiv:1709.09753 [physics.ins-det].

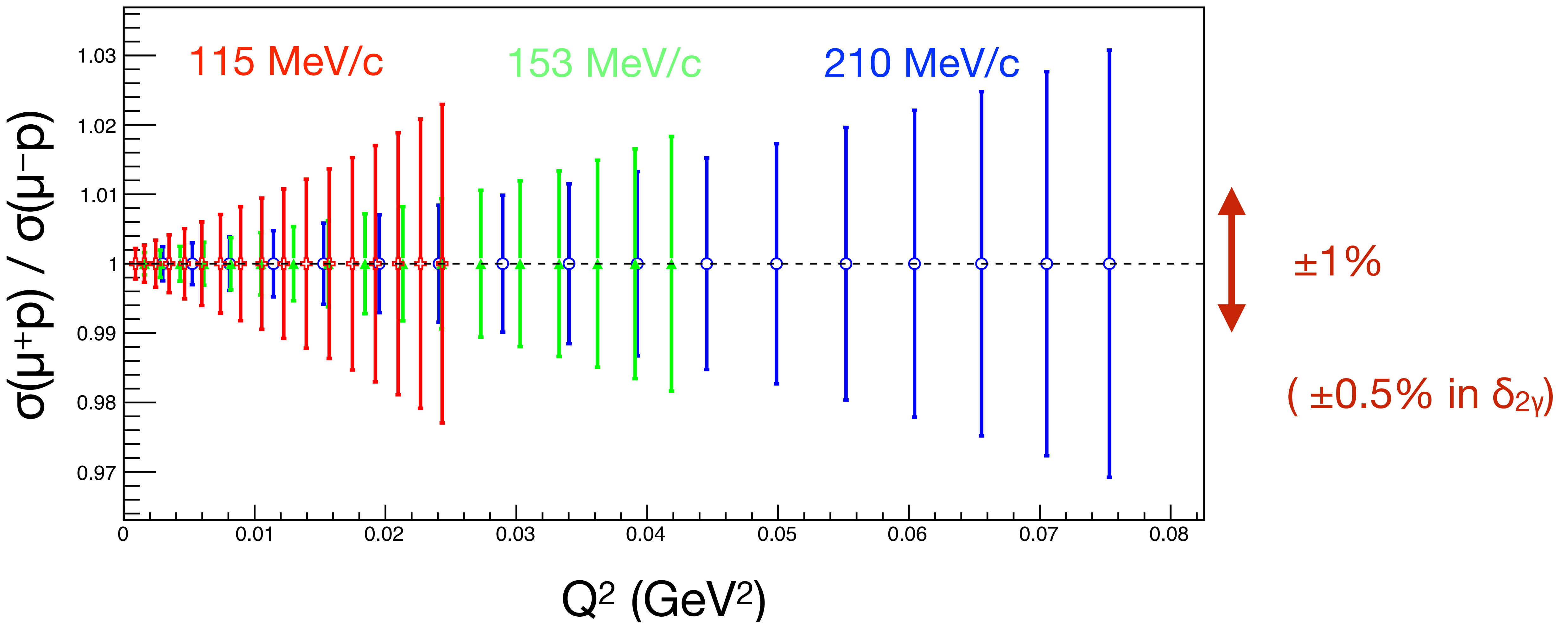

TPE correction at leading order, $\delta_{2\gamma}$

$$\sigma^{\pm} = \sigma_{1\gamma}(1 \pm \delta_{2\gamma})$$

$$\frac{\sigma^+}{\sigma^-} \approx 1 + 2\delta_{2\gamma}$$

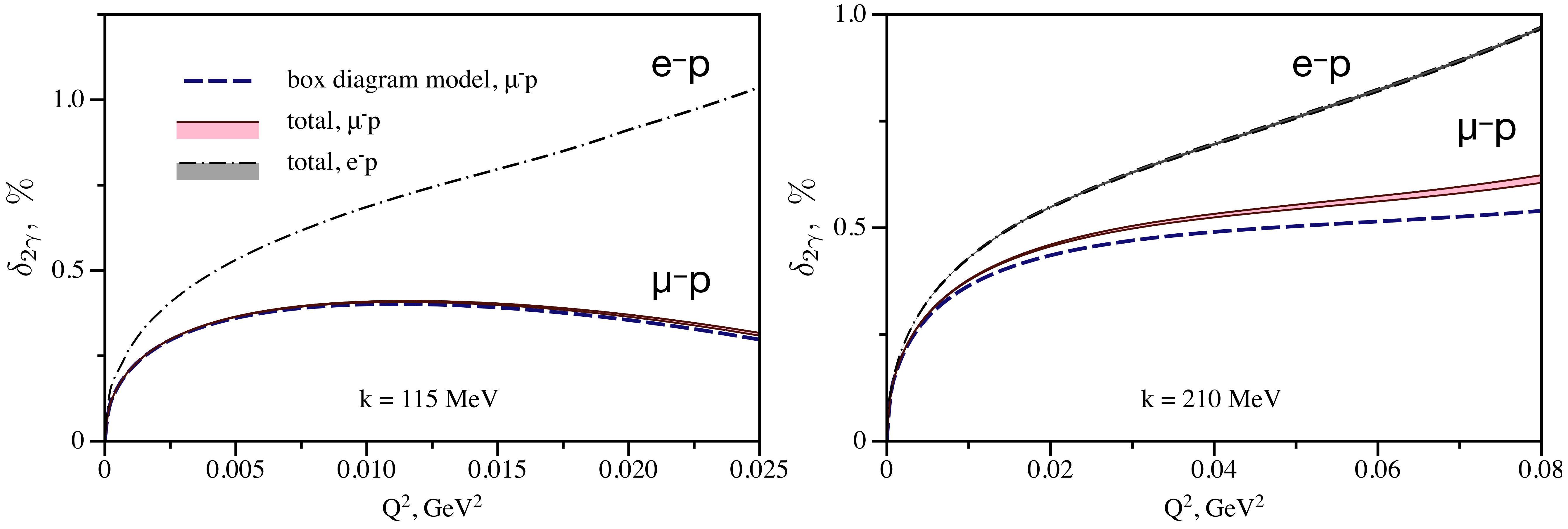

Prediction: Due to the cancellation of the helicity-flip and non-flip contributions, TPE in μp smaller than in ep.

Oleksandr Tomalak, Few-Body Systems, **59**, 87 (2018)

MUSE at the secondary beam line πM1

Beam

- 50 MHz RF (20 ns bunch separation)
- e, μ, π beams with large emittance
- Flux: 3.3 MHz
- Momentum: 115, 160, 210 MeV/c

Beam line detectors:

- Timing, identifying, and tracking of beam particles to the target and beyond

Scattered particle detectors:

- Timing and tracking of scattered particles with large solid-angle coverage

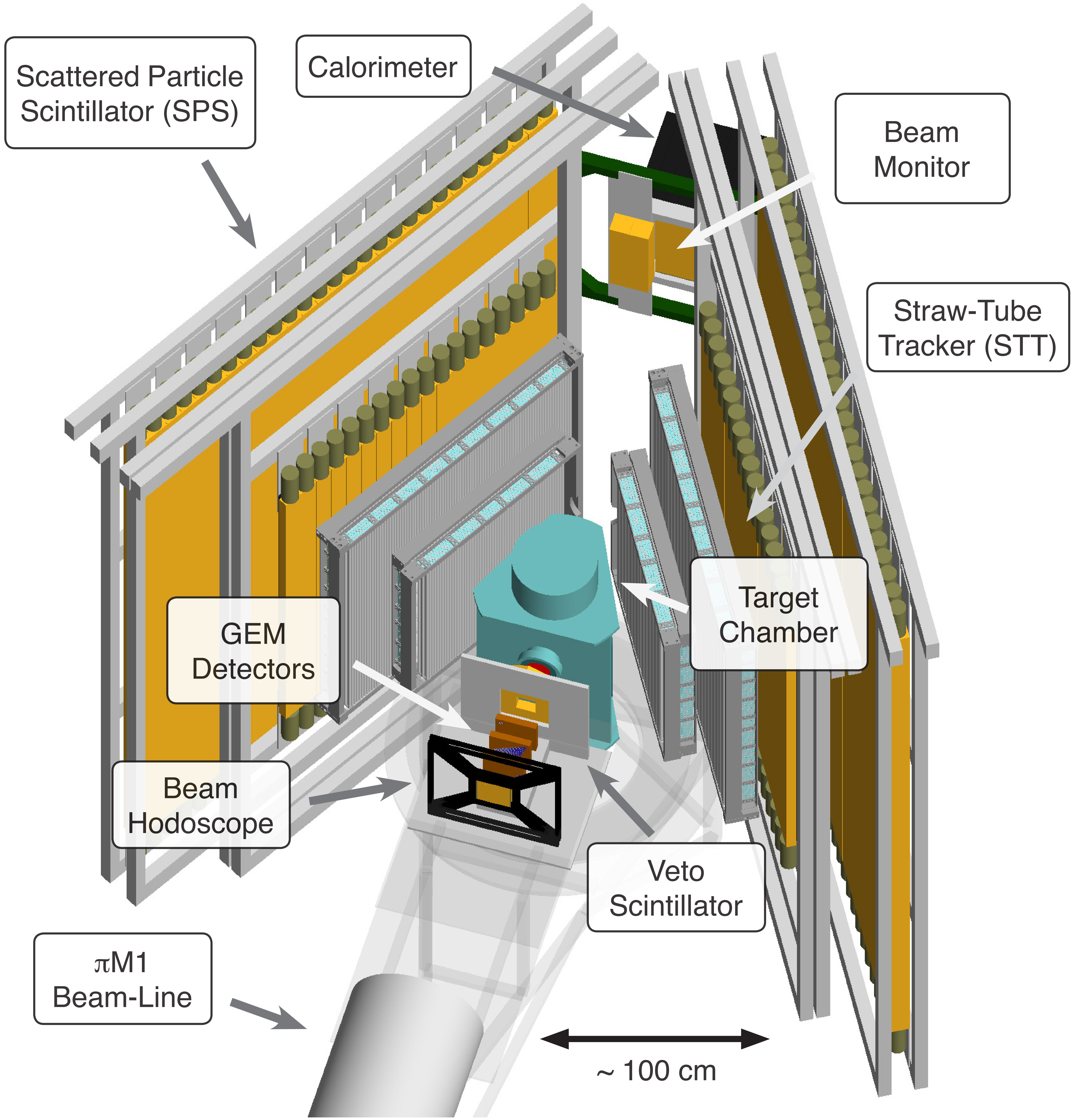

The MUon Scattering Experiment at PSI (MUSE), MUSE Technical Design Report, arXiv:1709.09753 [physics.ins-det].

Radiative corrections needed to obtain Born cross-section

Experimental Bremsstrahlung cross-section

$$\frac{d\sigma^{exp}}{d\Omega_l}(p'_{l,min}) = \int_{p'_l}\int_{\Omega_\gamma} \frac{d\sigma_{\text{brems}}}{d\Omega_l d\Omega_\gamma dp'_l} d\Omega_\gamma dp'_l$$

Born cross-section

$$\frac{d\sigma^{exp}}{d\Omega_l}(p'_{l,min}) = \frac{d\sigma_0}{d\Omega_l}\left[1 + \delta(p'_{l,min})\right]$$

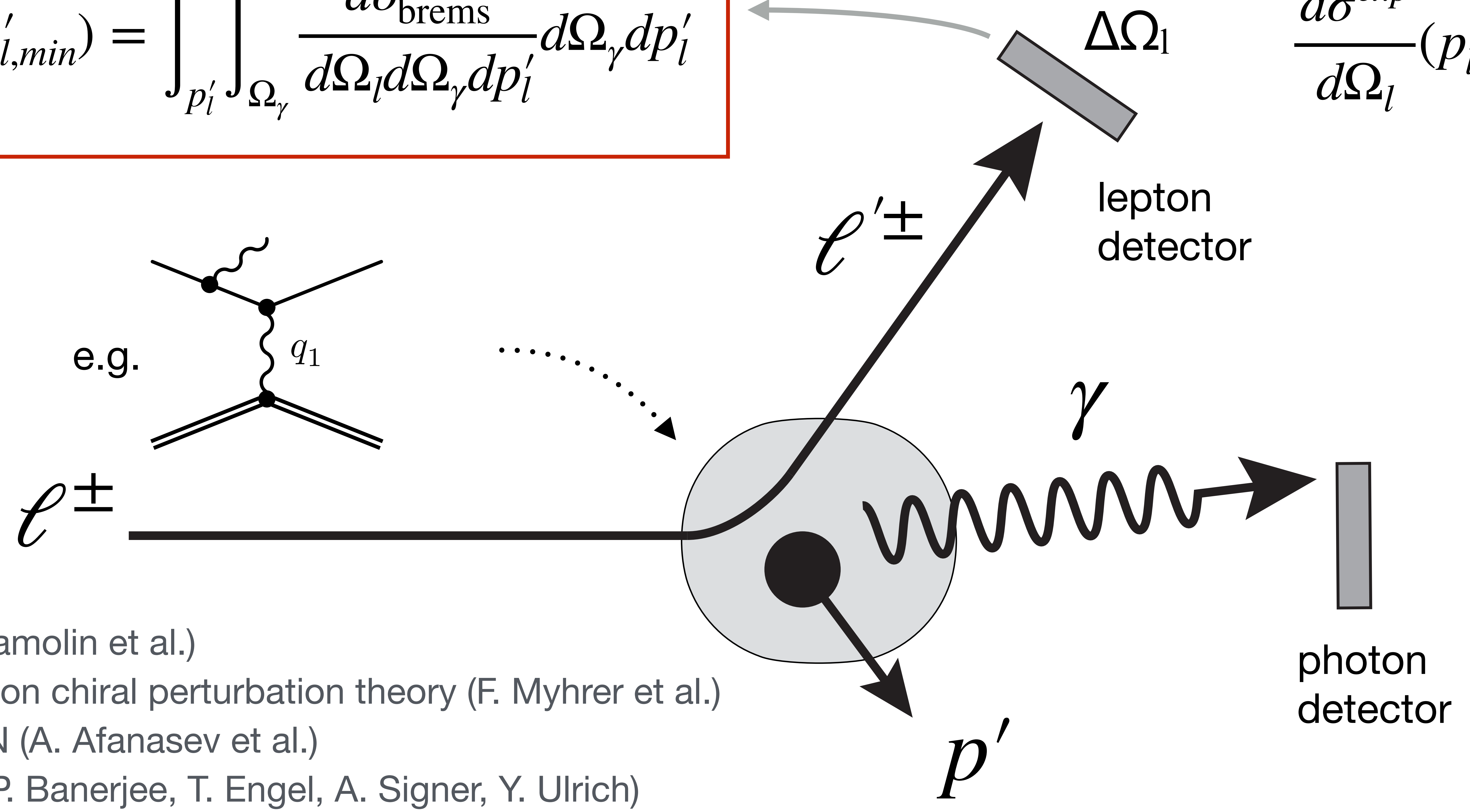

Radiative correction

$$\delta = \frac{d\sigma^{exp}}{d\Omega_l} / \frac{d\sigma_0}{d\Omega_l} - 1$$

ESEPP (Gramolin et al.)
Heavy baryon chiral perturbation theory (F. Myhrer et al.)
ELRADGEN (A. Afanasev et al.)
McMULE (P. Banerjee, T. Engel, A. Signer, Y. Ulrich)
…

Elastic Scattering of Electrons and Positrons on Protons (ESEPP)

first Born approximation

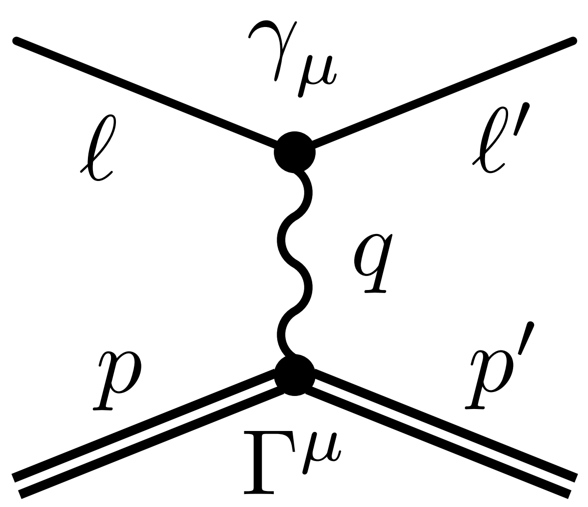

first-order bremsstrahlung processes $l^{\pm}p \to l'^{\pm}p'\gamma$

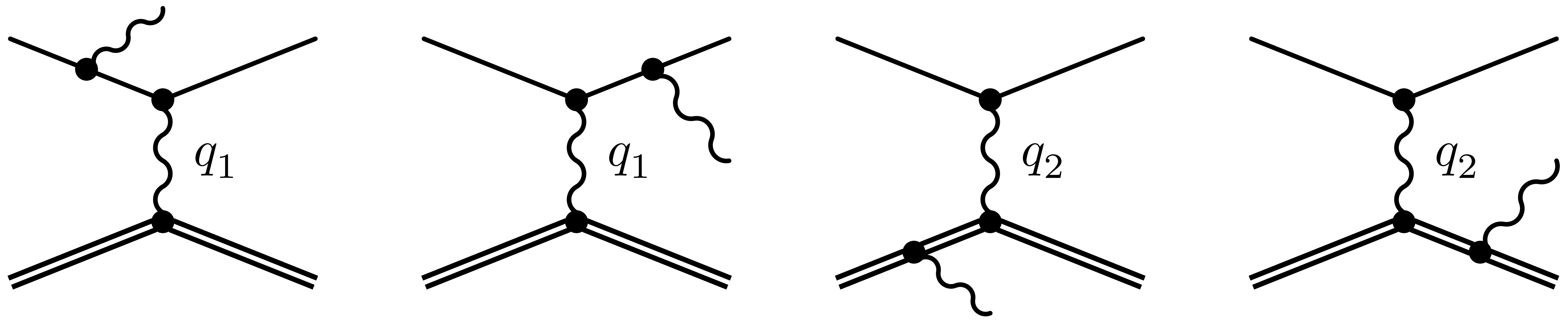

virtual-photon corrections

vacuum polarization

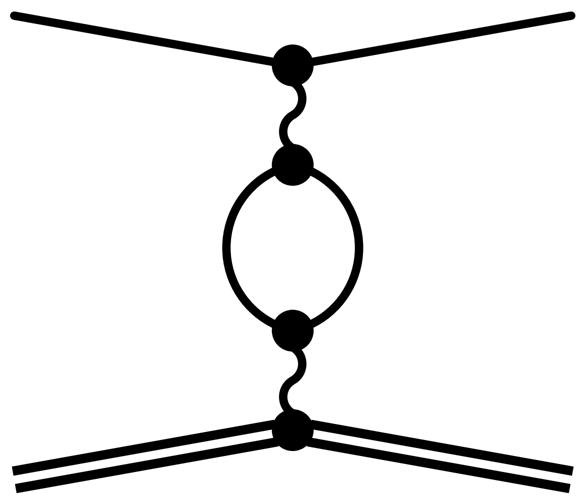

lepton/proton vertex corrections

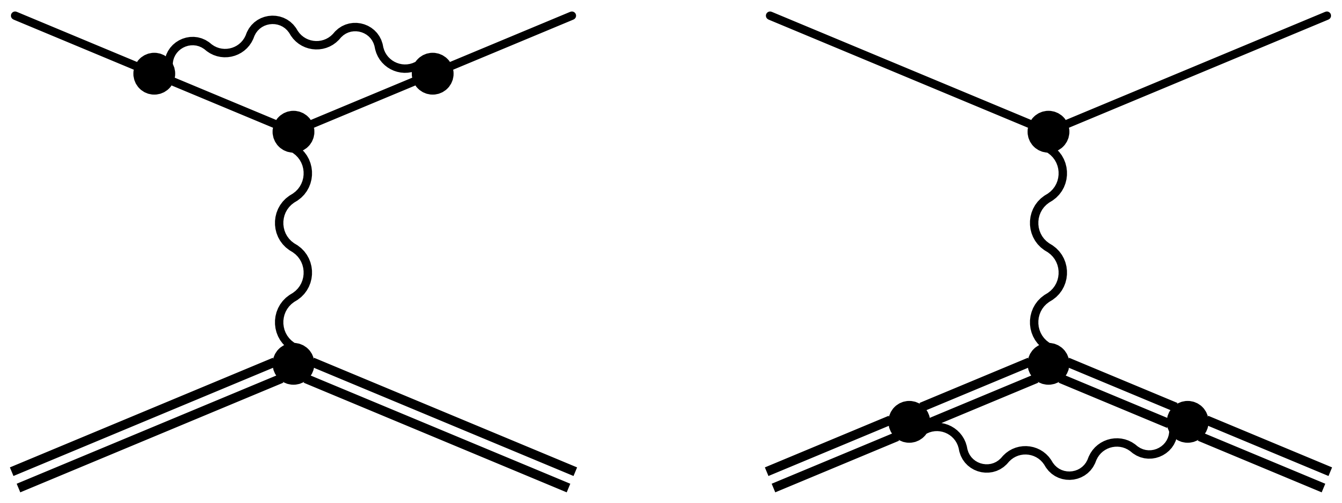

TPE corrections

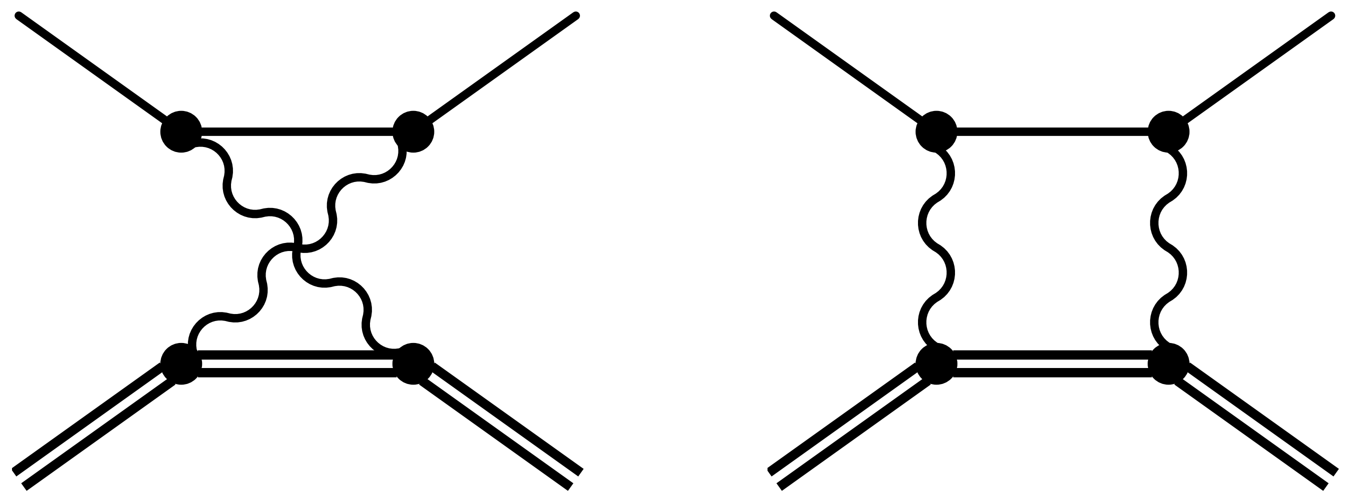

ESEPP includes emission of **hard radiated photon**, beyond soft-photon approximation and the **mass of lepton**.

A.V. Gramolin et al., J. Phys. G: Nucl. Part. Phys. 41 (2014) 115001 (28pp)

The ESEPP event generator

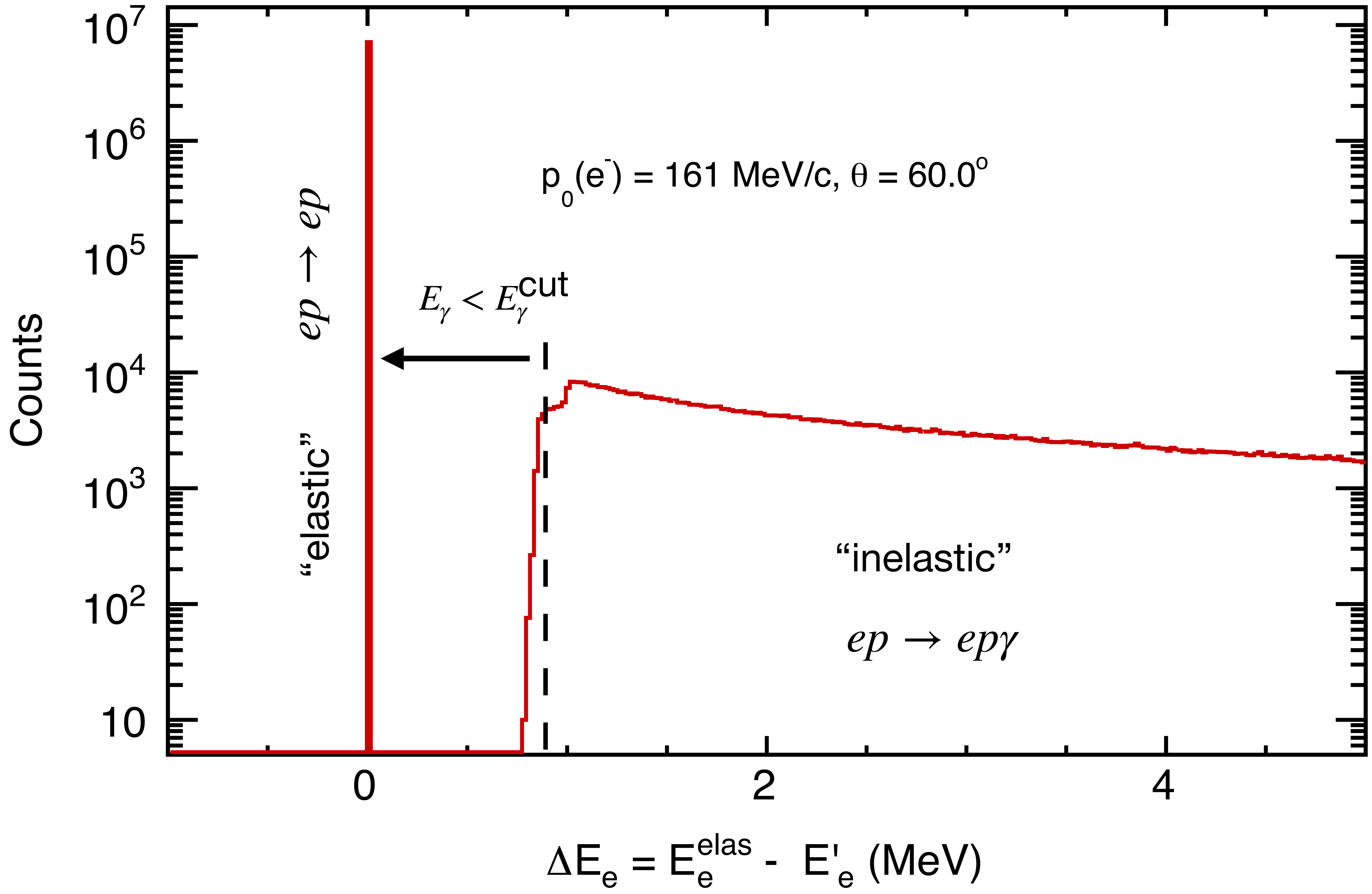

- ESEPP generates unweighted events
- Two types of events: elastic (analytical integration) and inelastic (numerical integration)
- First-order bremsstrahlung is taken into account in both cases

A.V. Gramolin et al., J. Phys. G: Nucl. Part. Phys. 41 (2014) 115001 (28pp)

Bremsstrahl cross section from ESEPP in MUSE kinematics

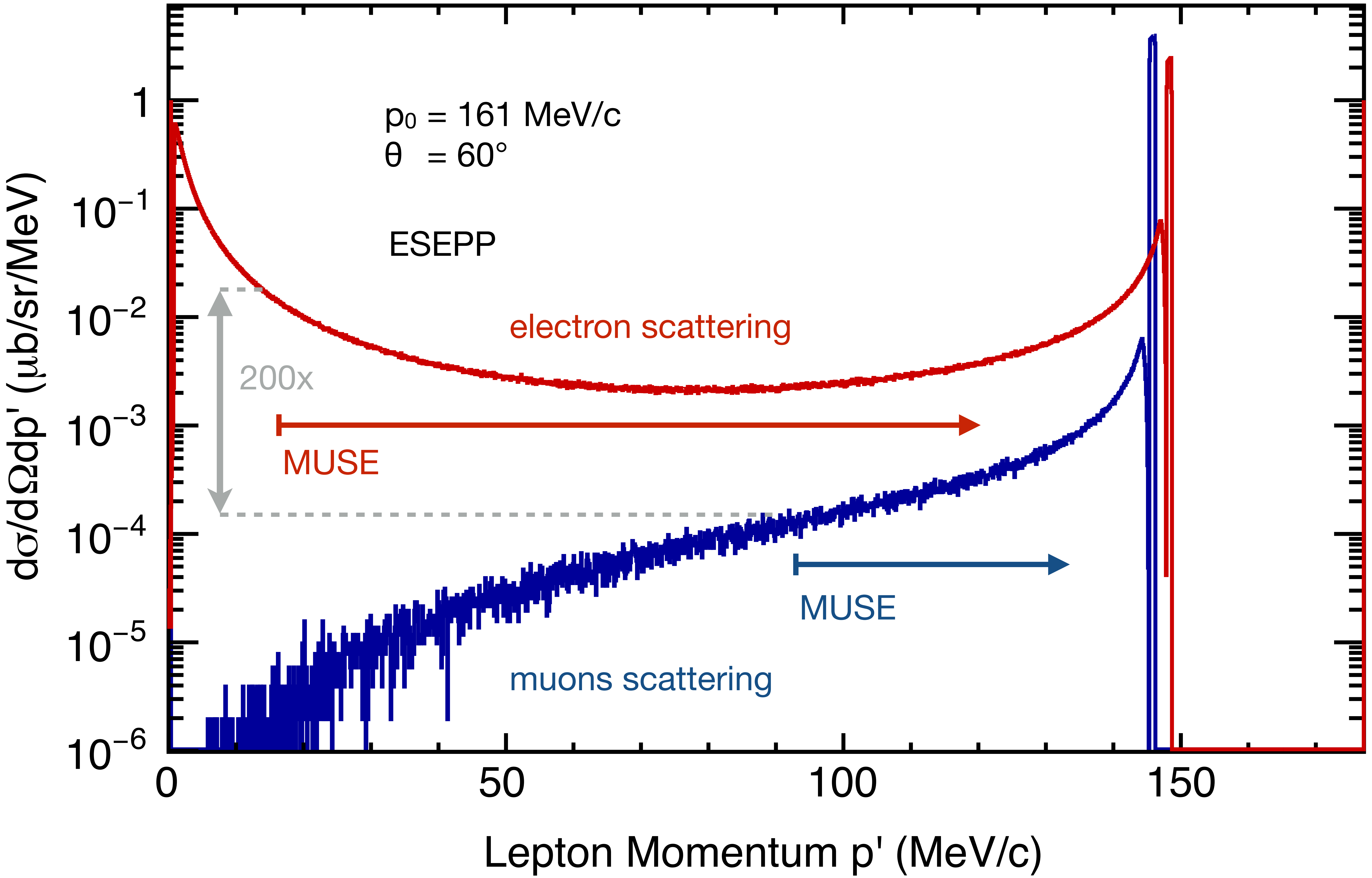

Radiative tail spectrum

Low-energy lepton-proton bremsstrahlung via effective field theory

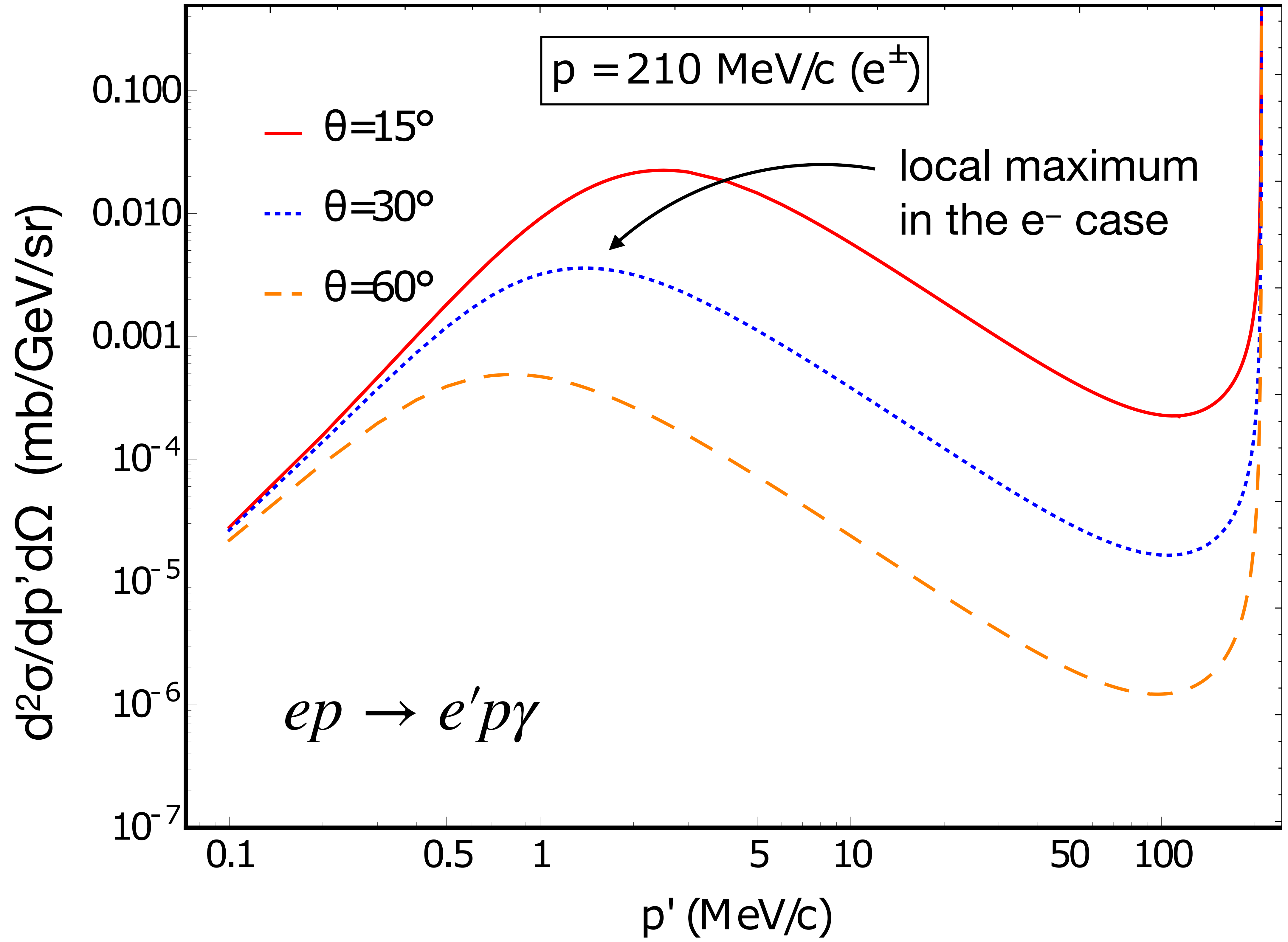

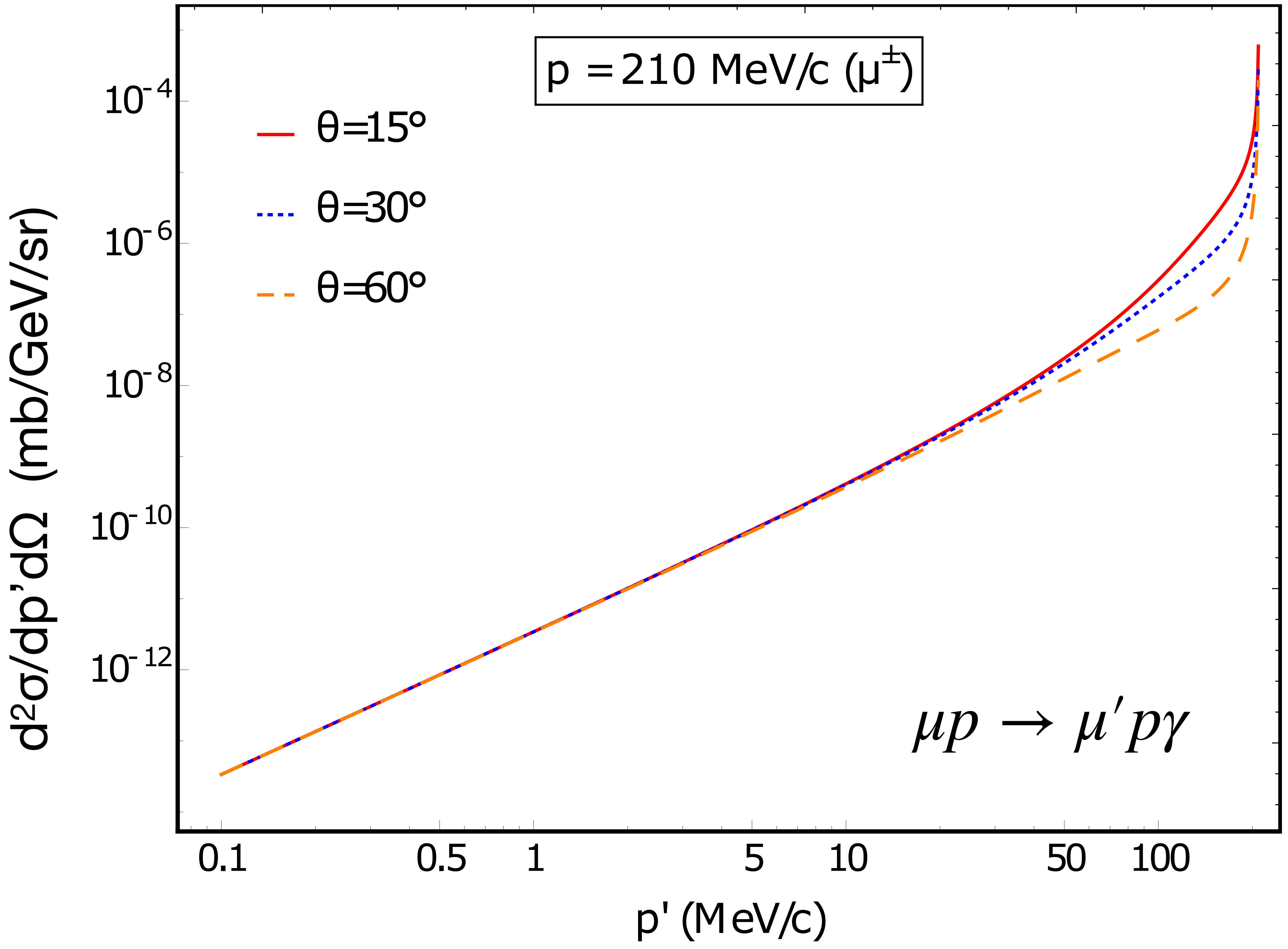

P. Talukdar, F. Myhrer, G. Meher, and U. Raha, Eur. Phys. J. A (2018) **54**: 195.

$ep \to e'p\gamma$ Cross section in MUSE kinematics

MUSE will integrate over a large momentum range

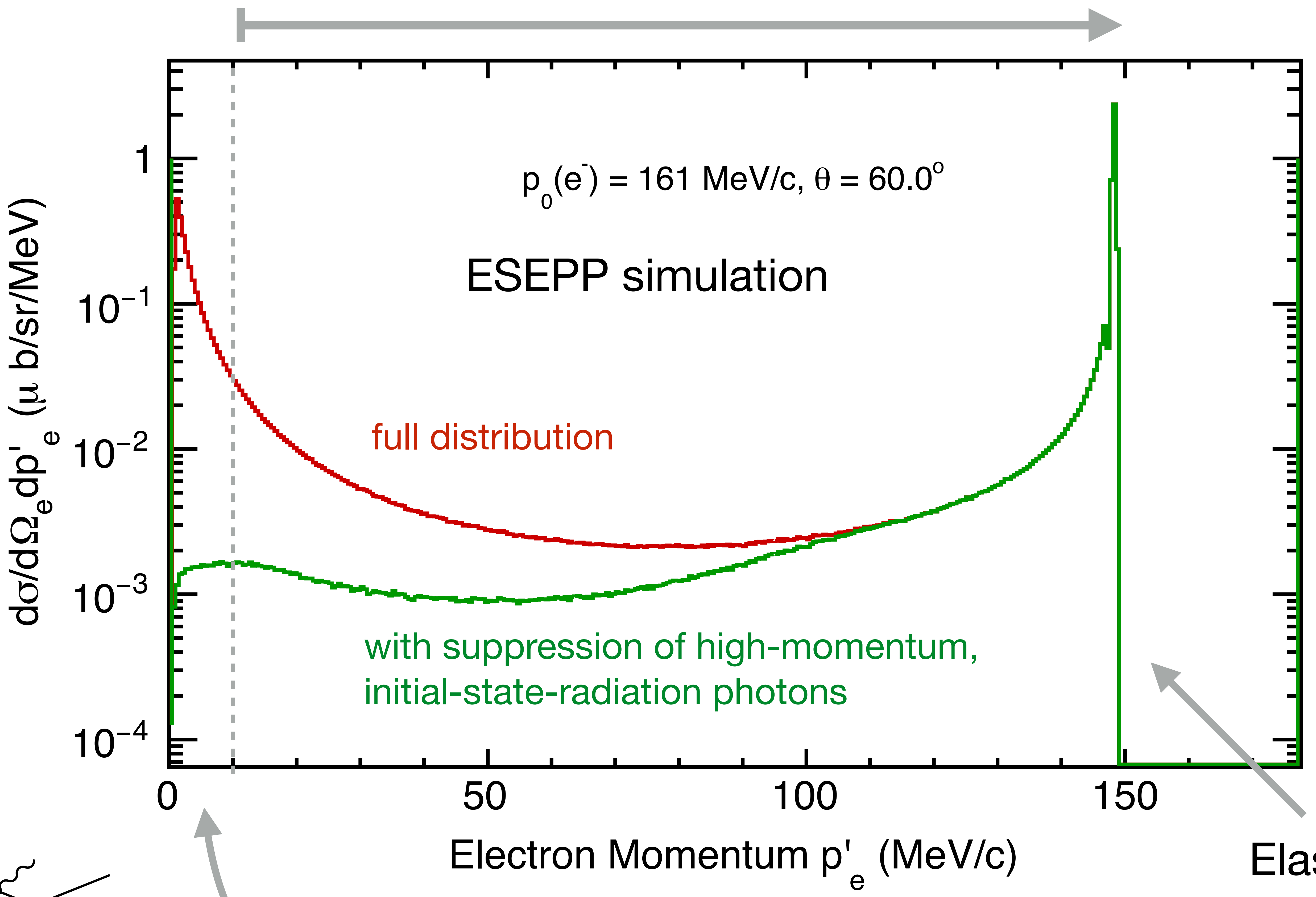

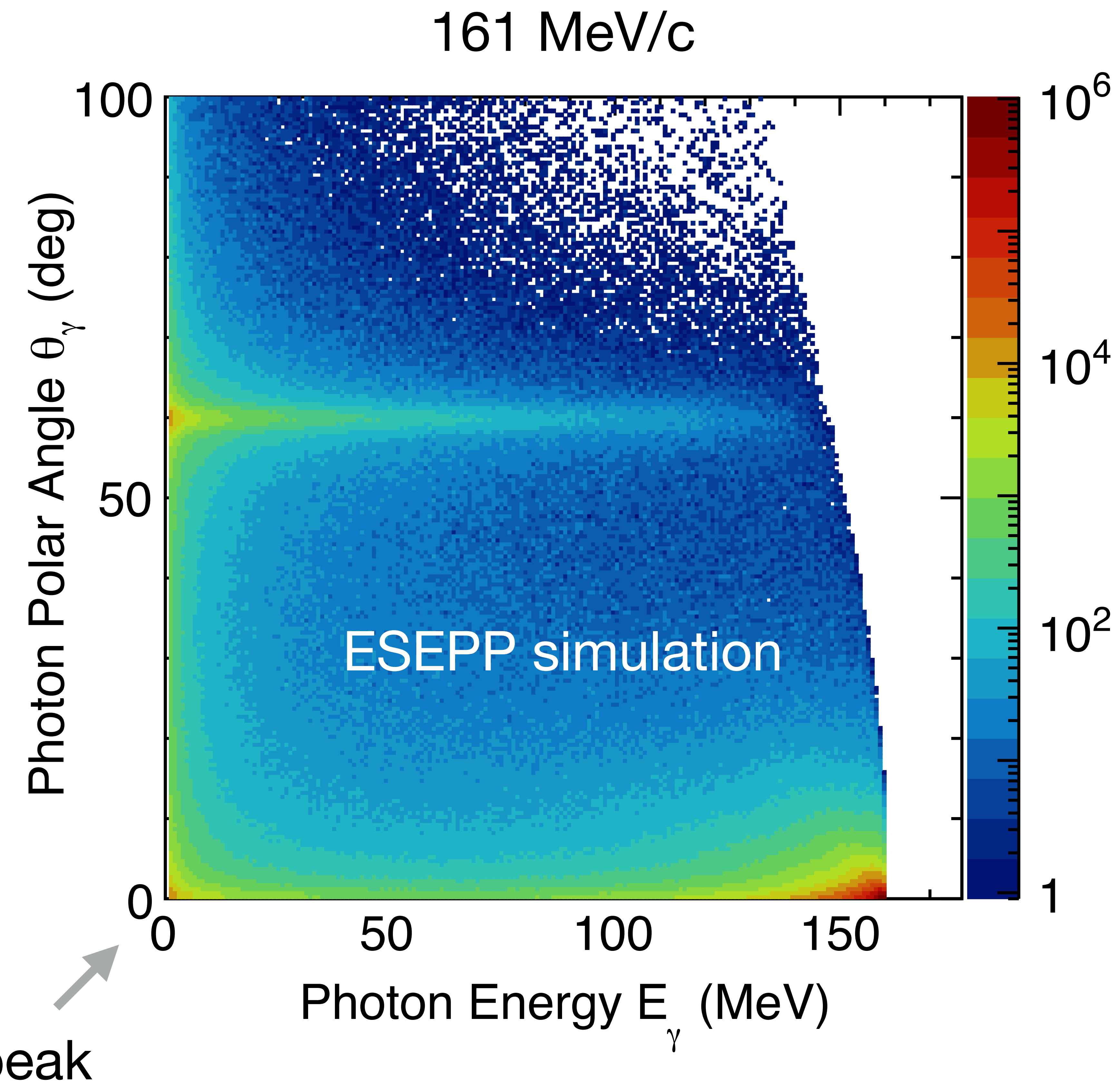

Elastic peak

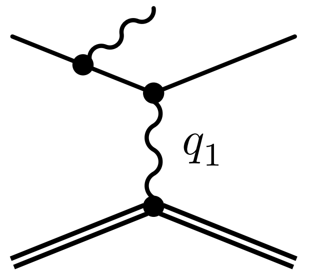

If the incident lepton loses energy due to the emission of a hard photon, then the probability for this lepton to be scattered by the proton increases.

ESEPP events in the MUSE setup

$p_0 = 161$ MeV/c

$\theta \approx 60^\circ$

Examples: $ep \rightarrow e'p\gamma$

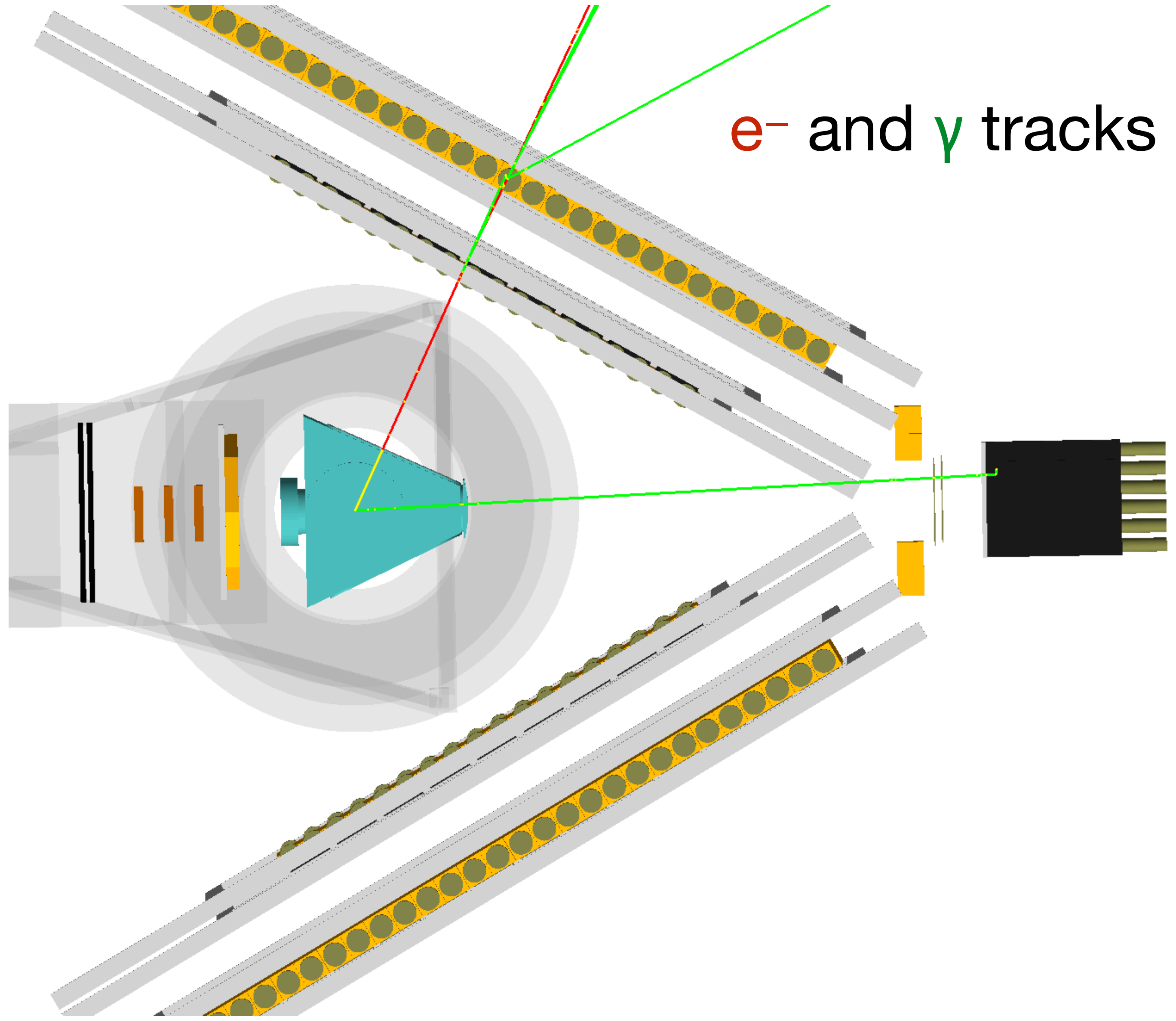

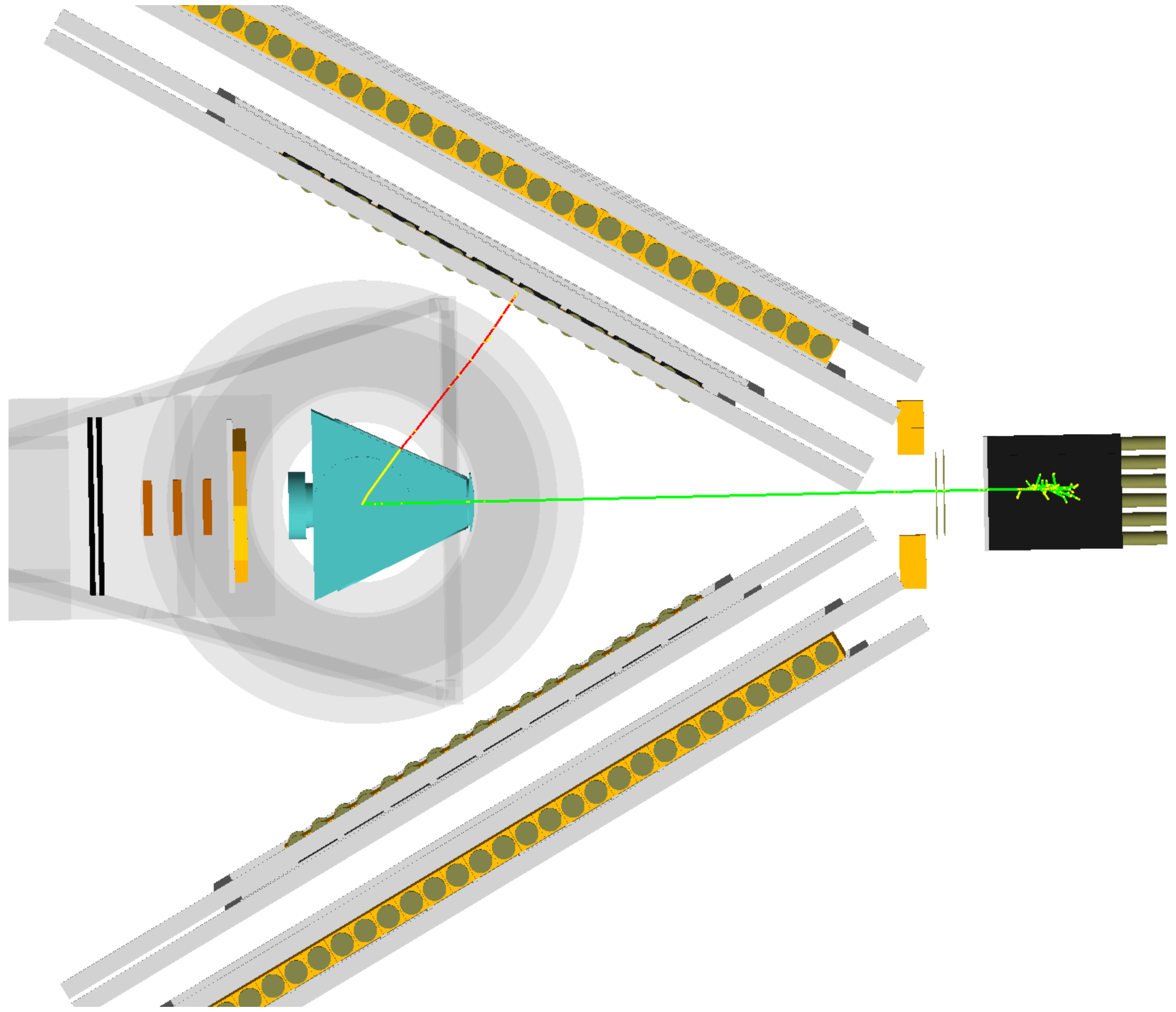

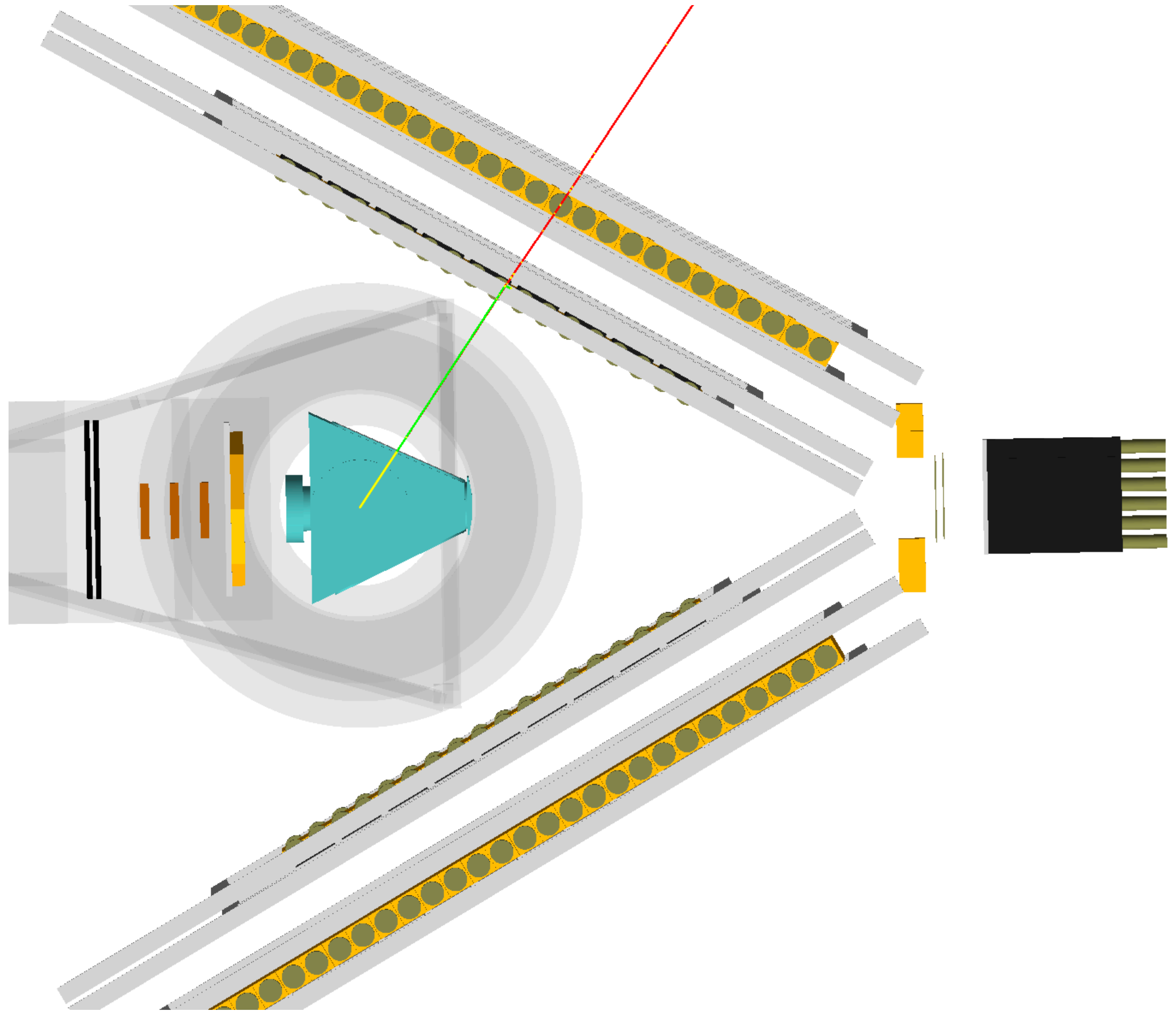

Initial-state radiation
low photon energy

$p'_e > p'_{min}$

Initial-state radiation
high photon energy

$p'_e < p'_{min}$

Final-state radiation

The size of the radiative corrections depends on the detector properties and event selection

$$\delta = \delta(p_0, \theta_l, p'_{min}, \Omega_\gamma)$$

- kinematics of elastic scattering
- experimental conditions
- event selections

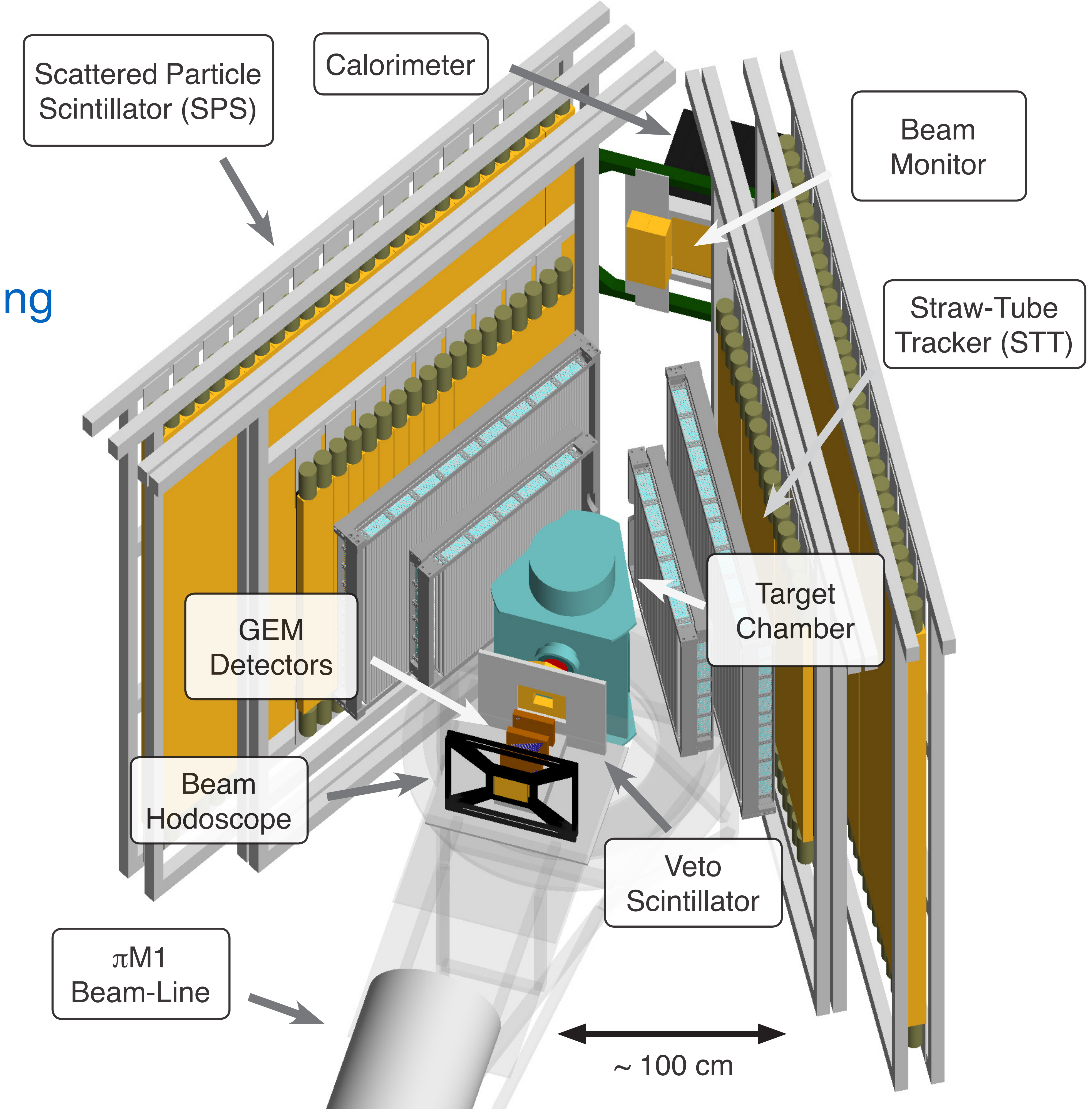

Scattered lepton (GEM, STT, SPS)

- angular acceptance
- particle momentum (magnitude not precisely measured)

Internal Bremsstrahlung (CAL)

e.g., initial-state radiation

Incident lepton (TOF)

- beam momentum
- multiple scattering
- external Bremsstrahlung

Recoiling proton

remains unobserved

MUSE detector system for TOF measurements

$$\delta = \delta(p_0, \theta_l, p'_{min}, \Omega_\gamma)$$

$$\beta_i^{\mu,\pi} = \frac{L}{ct} = \frac{t_i^e - t_0^e}{t_i^{\mu,\pi} - t_0^{\mu,\pi}}$$

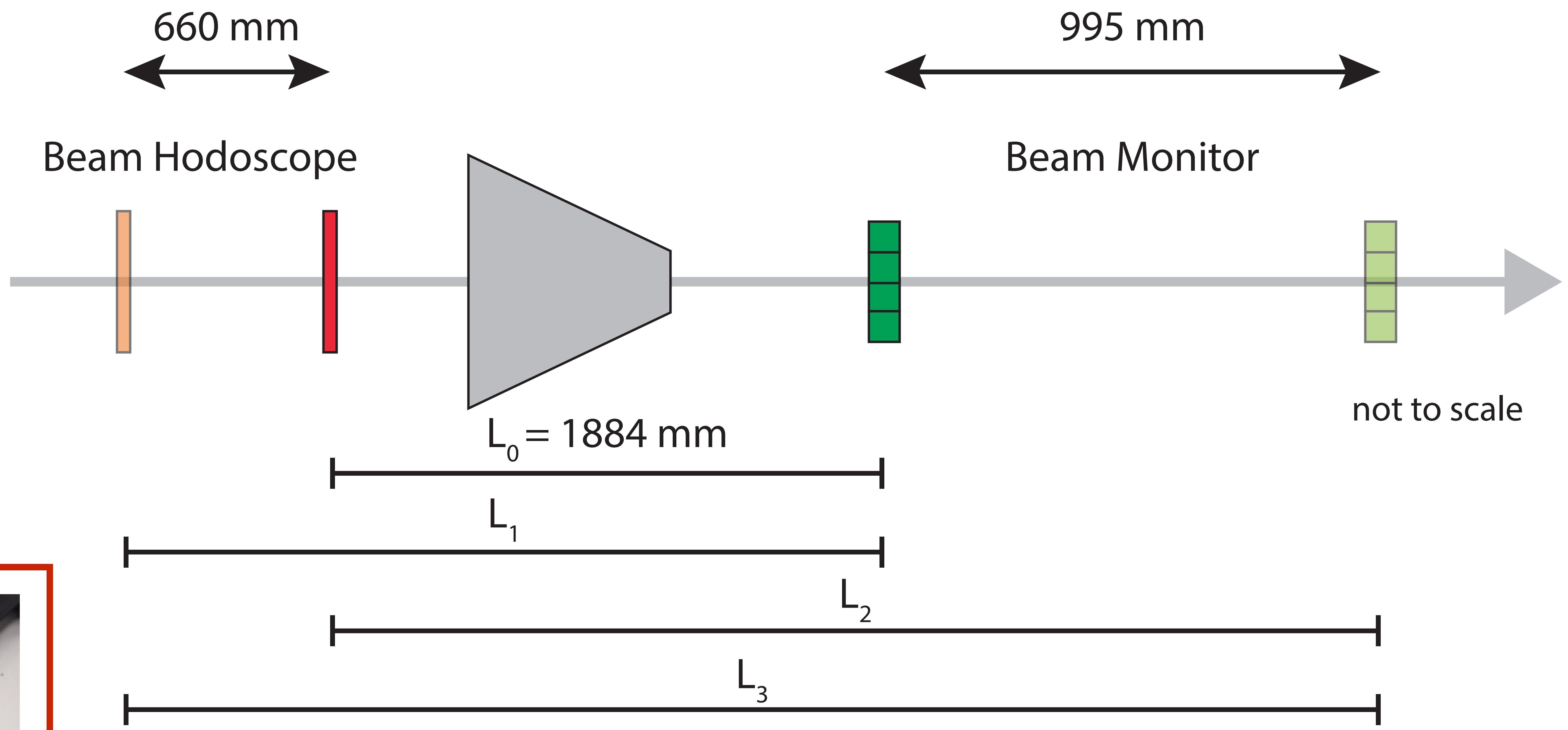

Beam monitor
SC bars in center

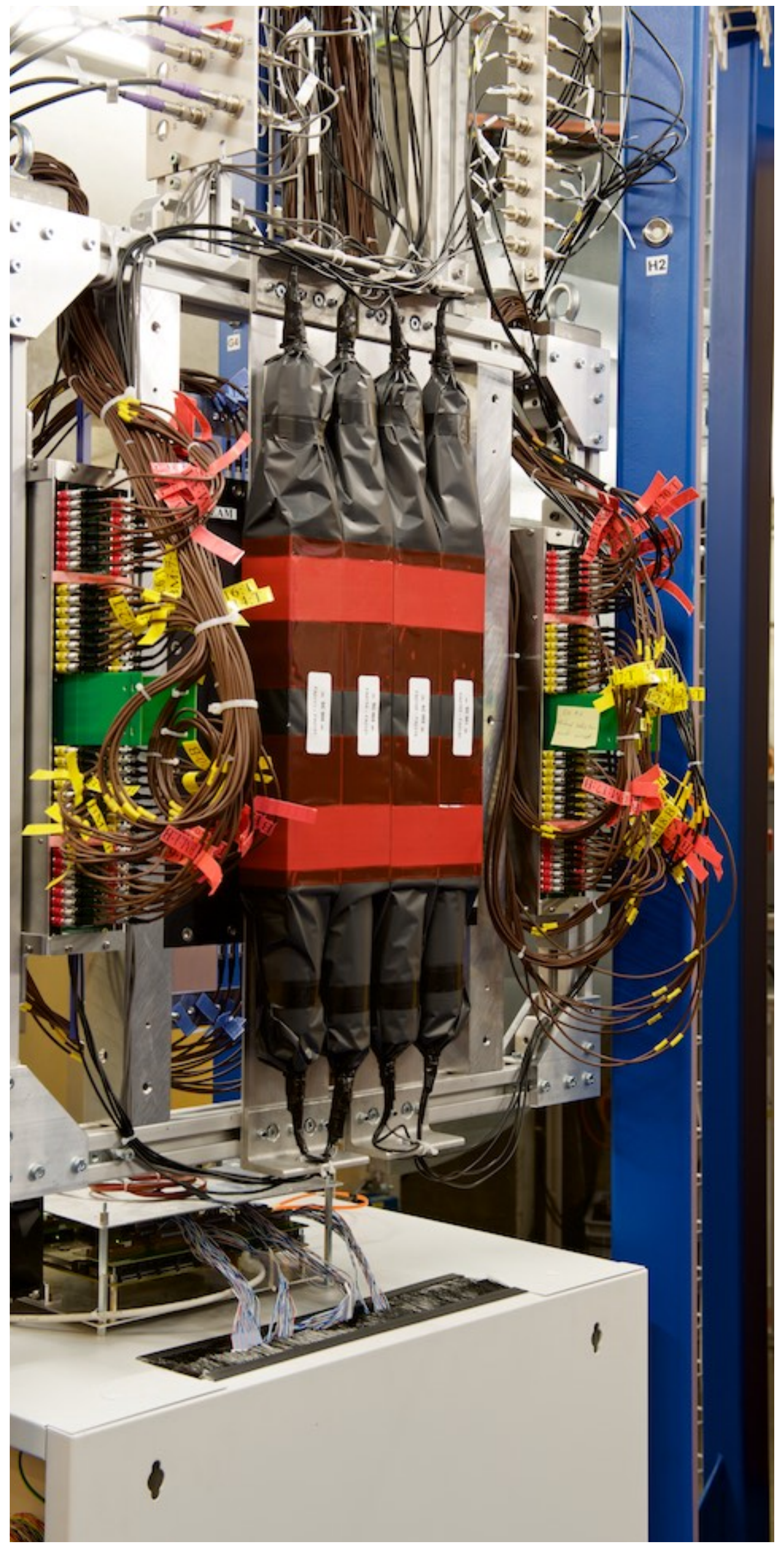

Beam hodoscope
planes C & D

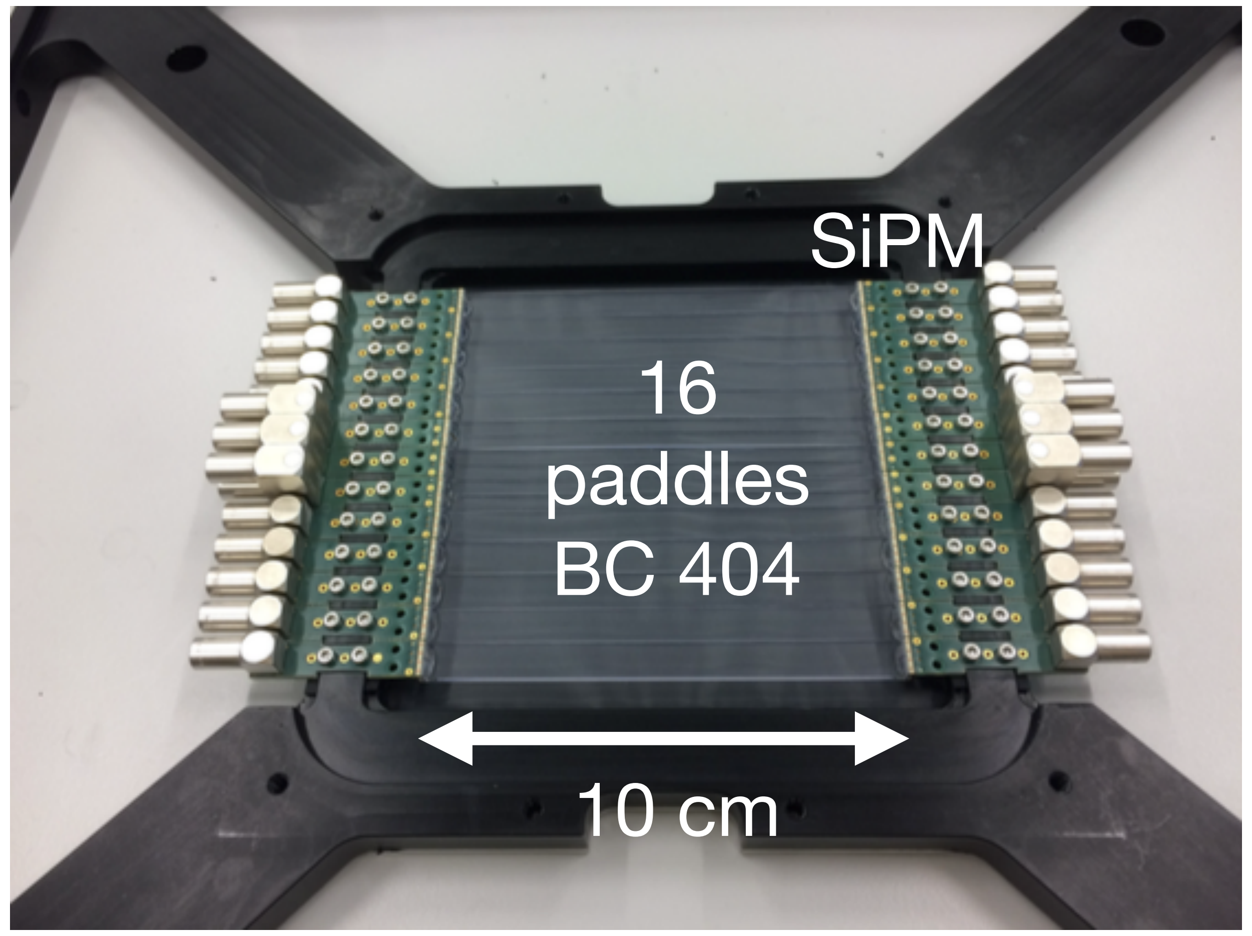

Electron time-of-flight provides **path length** information.

Measure the μ and π average particle speeds over the paths L1, L2, and L3 to obtain **beam momenta**.

$$\sigma_{p_0} \approx 0.002 \cdot p_0$$

MUSE tracking detectors

GEM detectors (Hampton Univ.)

- Set of three GEM detectors.
- Measure trajectories into the target to reconstruct the scattering kinematics.

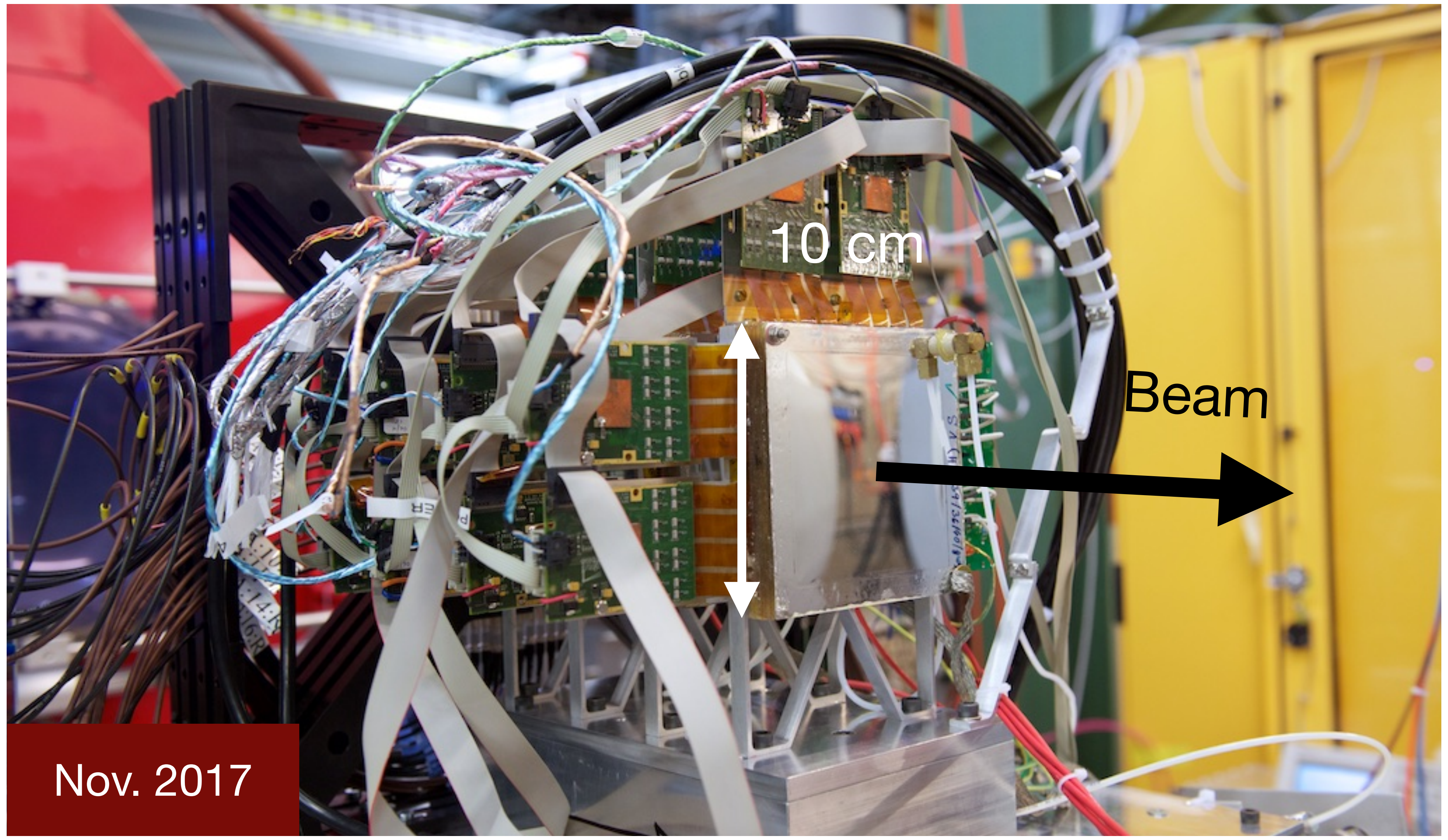

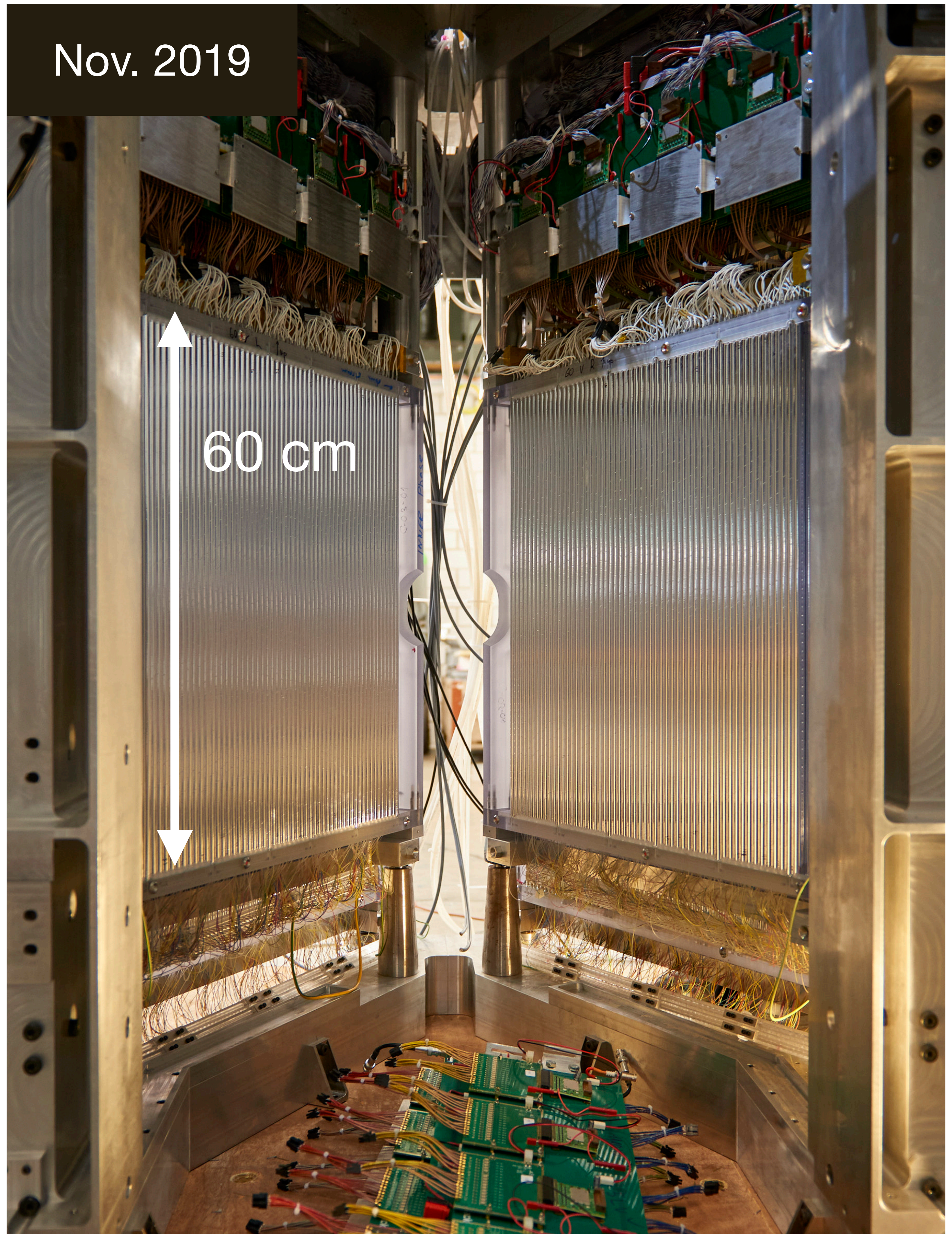

Straw-tube tracker
(Hebrew University of Jerusalem + Temple)

- Two STT chambers with 5 vertical and 5 horizontal planes each (3000 straws total).
- The Straw Tube Tracker provides high-resolution and high-efficiency tracking of the scattered particles from the target.

Reconstruction of scattering angle

$$\delta = \delta(p_0, \theta_l, p'_{min}, \Omega_\gamma)$$

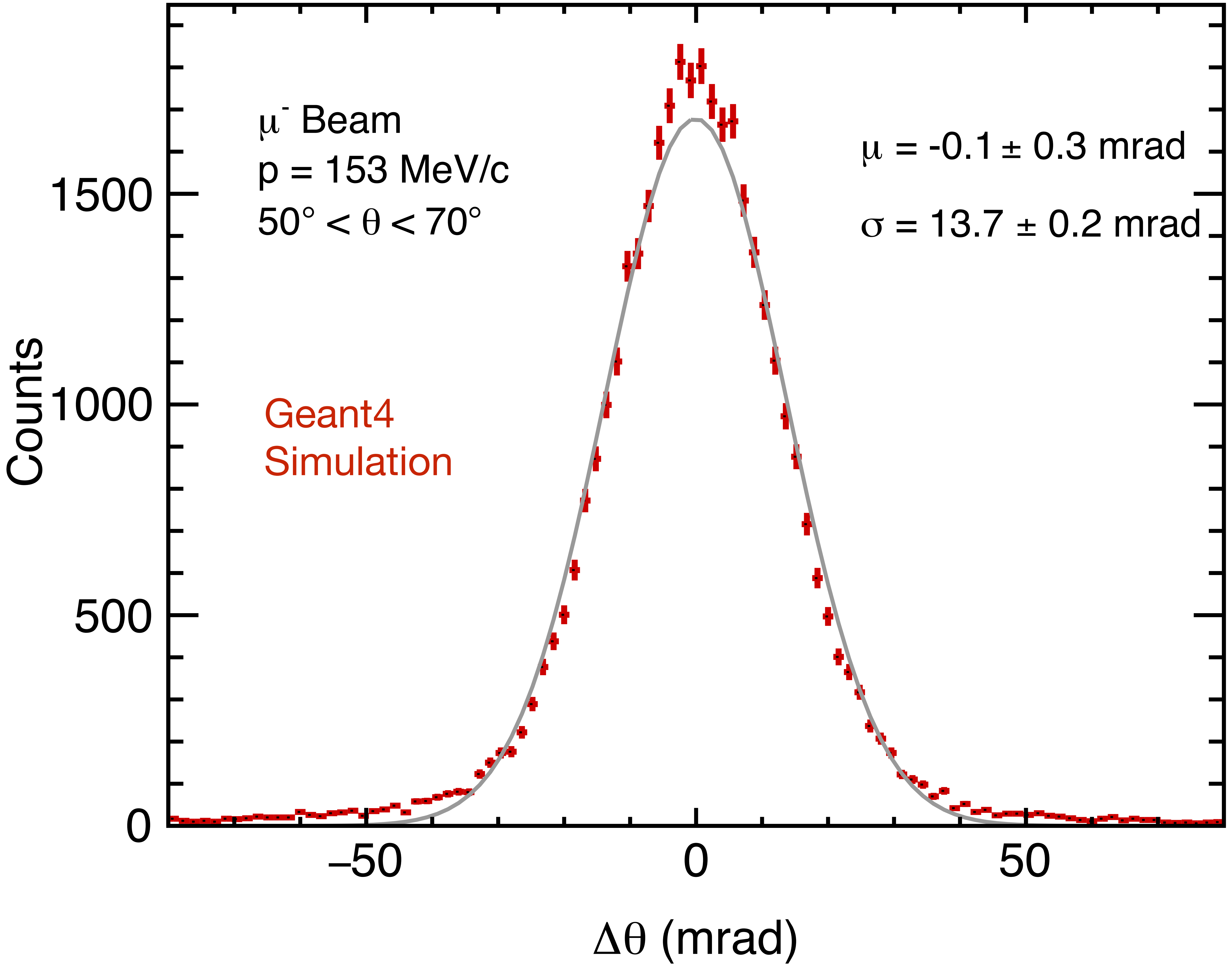

Position resolution:
GEM 70 μm and STT 120 μm.

Full Geant4 simulation including detector material and target.

Scattering-angular resolution for <u>one</u> event is dominated by multiple scattering and ≤ 20 mrad.

MUSE systematic uncertainties of the scattering angle is ≤ 1 mrad

$$\sigma_\theta < 1 \text{ mrad}$$

Scattered-particle scintillators as event trigger and for reaction ID

$\delta = \delta(p_0, \theta_l, p'_{min}, \Omega_\gamma)$

Front wall: 18 bars (6 cm x 3 cm x 120 cm)
Rear wall: 28 bars (6 cm x 6 cm x 220 cm)

Scattered-particle scintillators exceed required time resolution:
σ(Front) < 50 ps, σ(Rear) < 60 ps

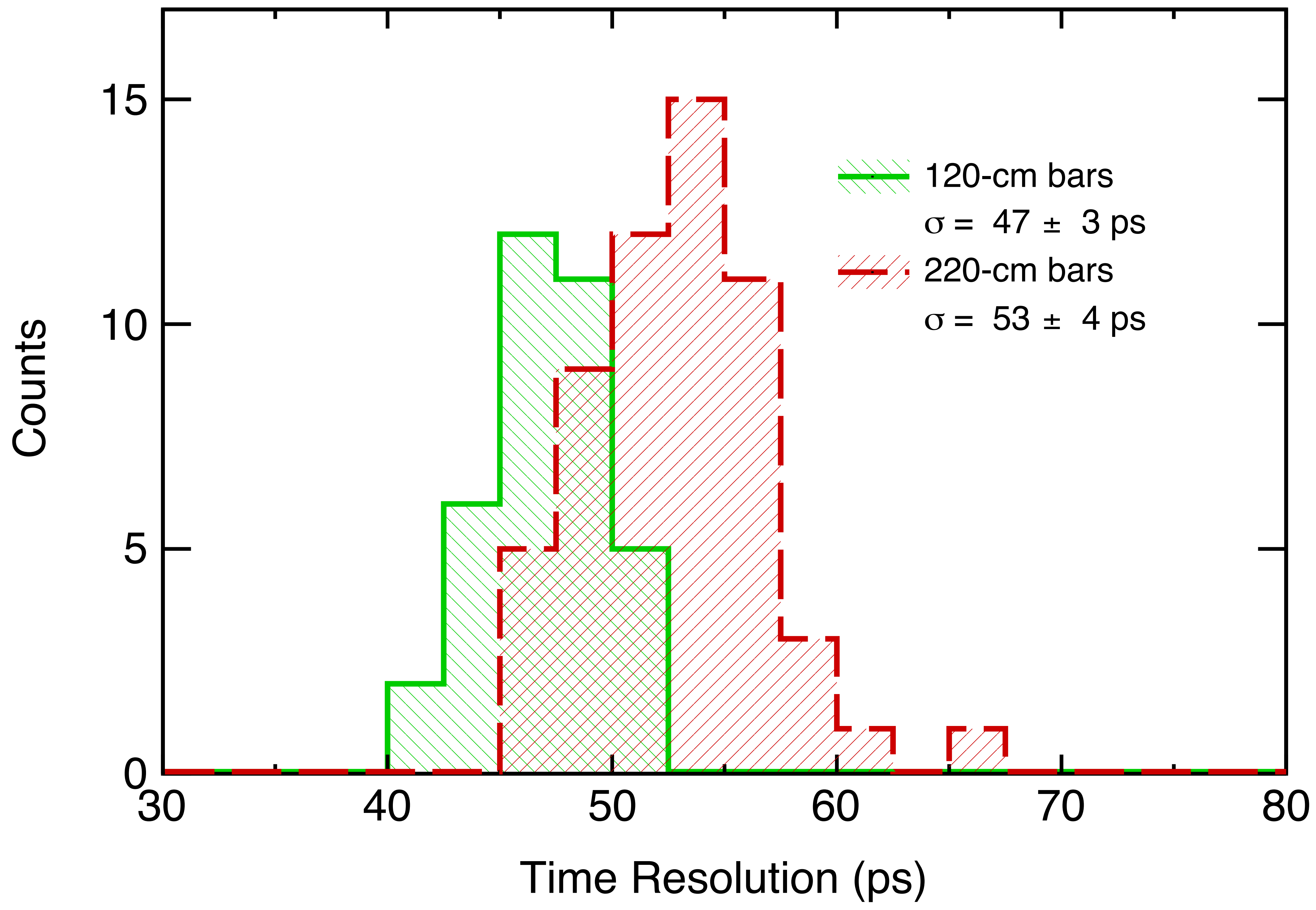

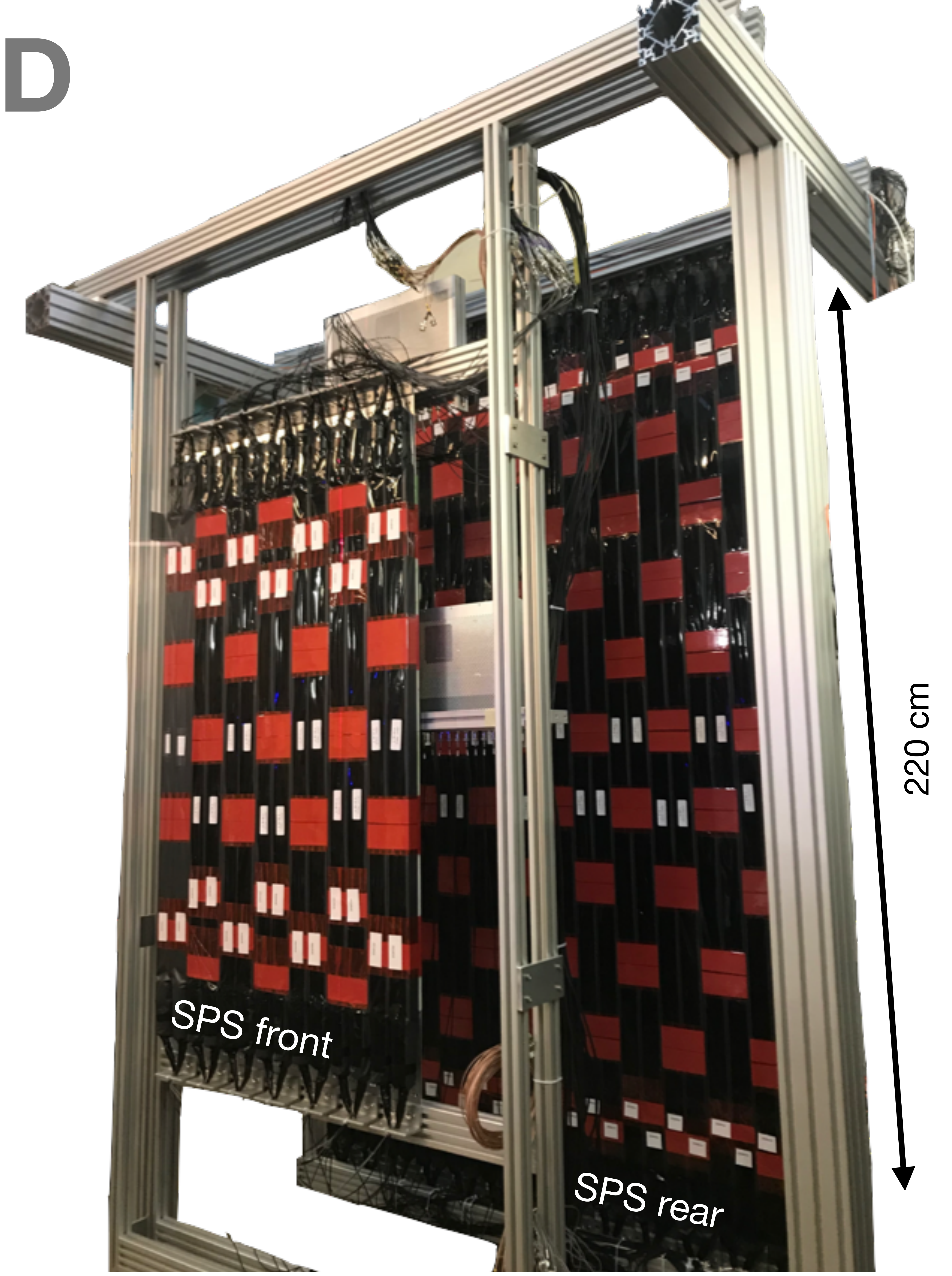

SPS detector in test stand

Confirmation of ^{208}Tl Gamma calibration of SPS bars

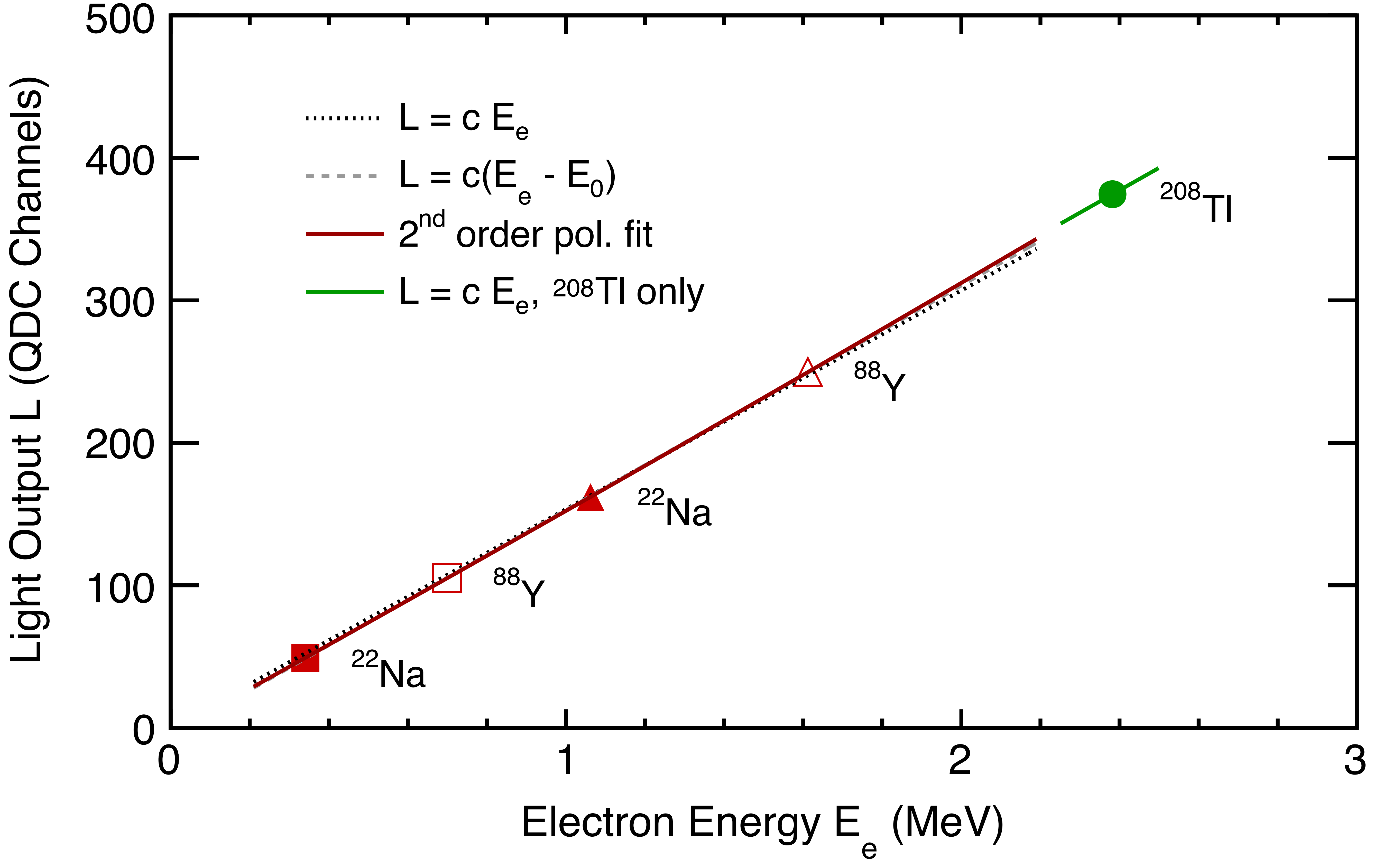

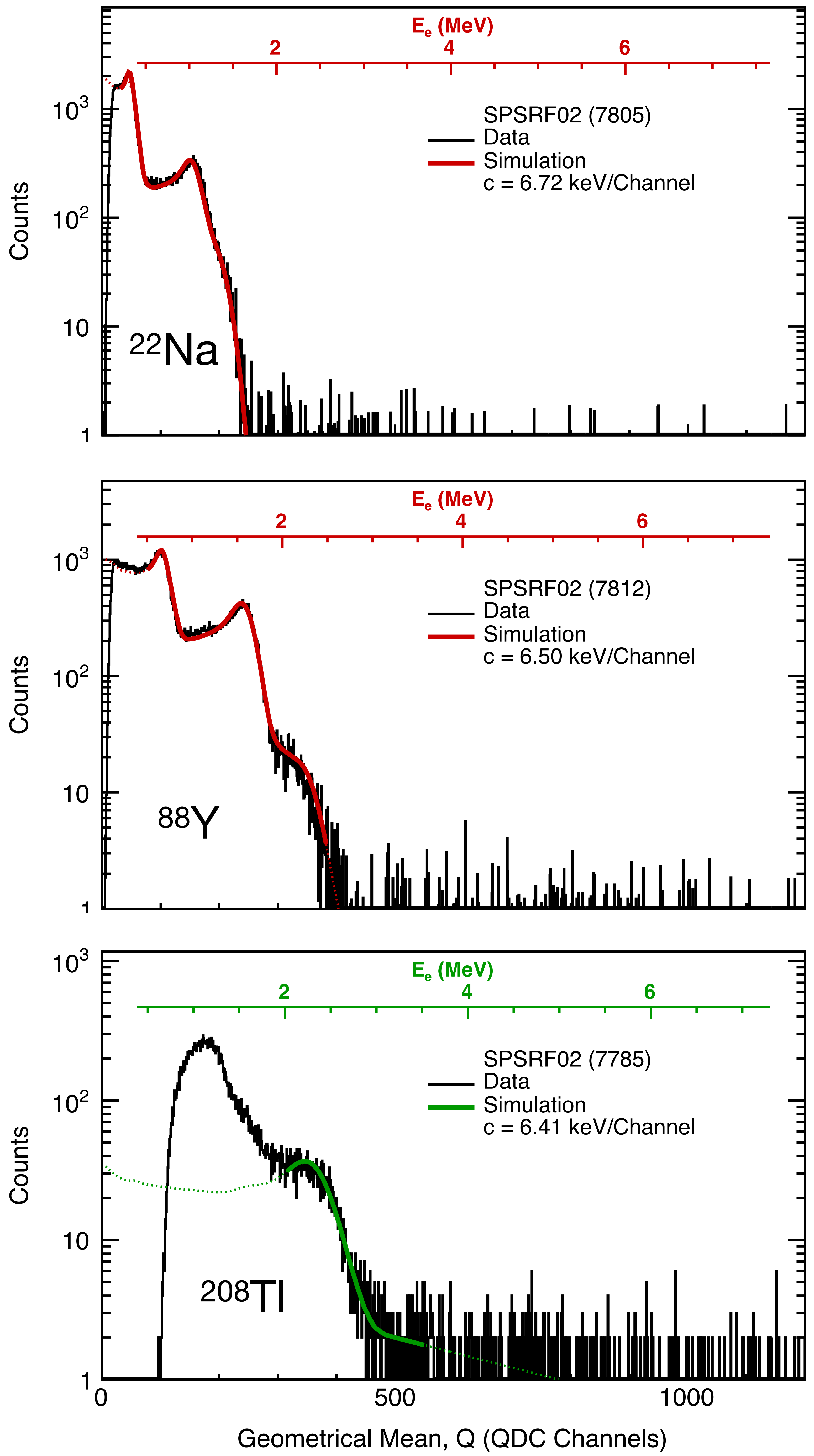

Calibrations with room background ^{208}Tl agree with source-data (^{22}Na and ^{88}Y) results to better than 1% at the anticipated SPS threshold of 2 MeV.

Electron detection threshold in the SPS

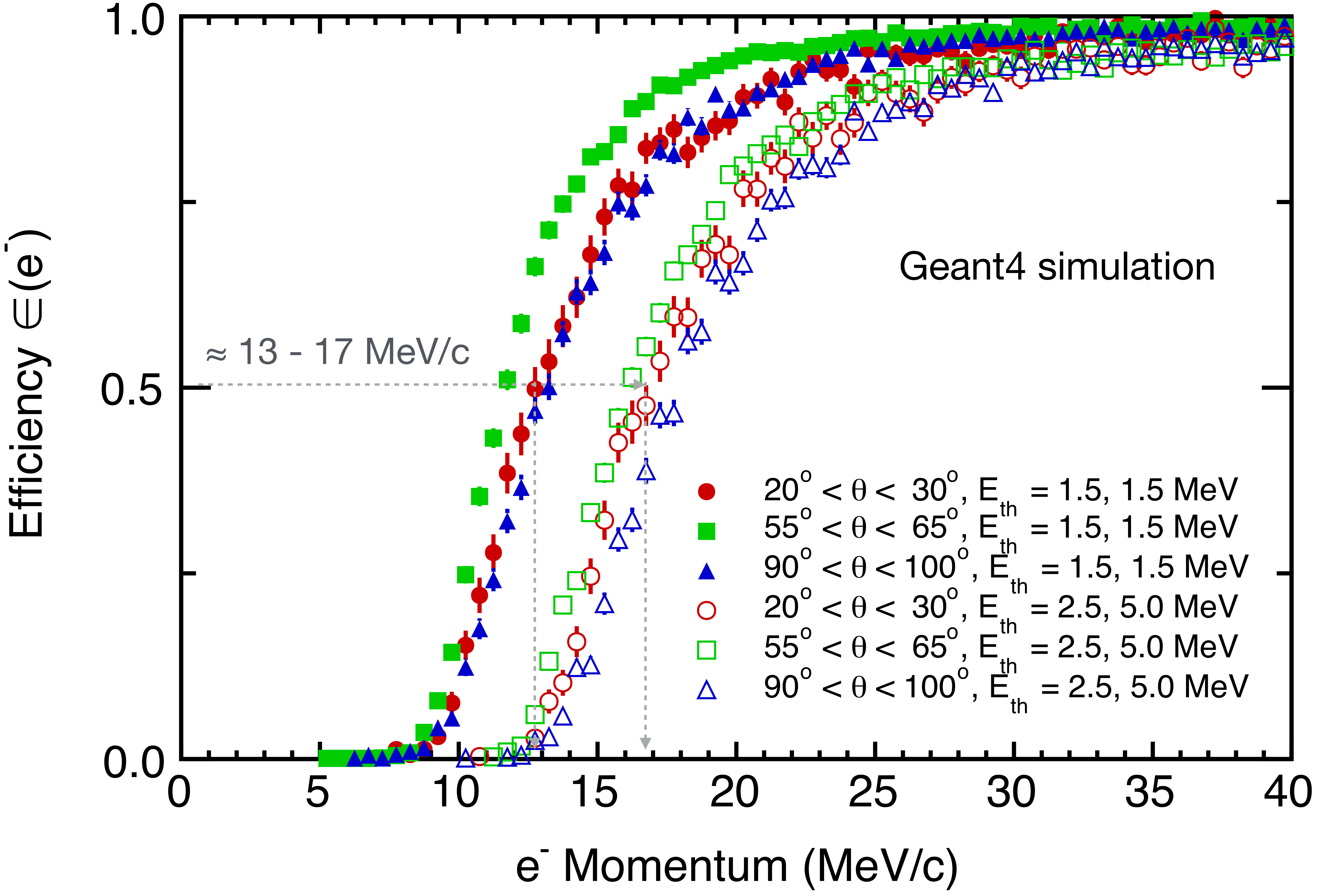

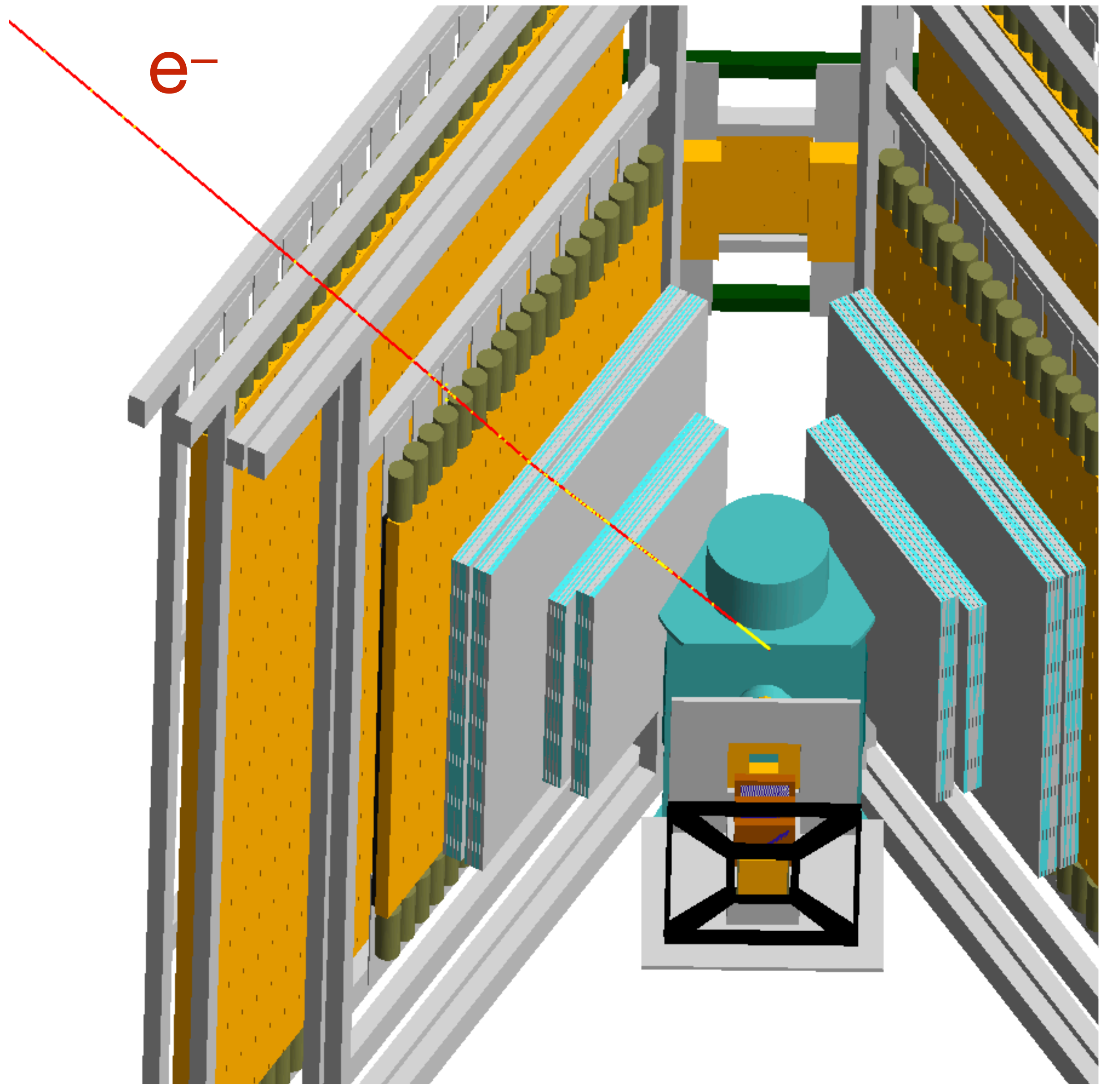

p'_{min} is primarily determined by the SPS detector:

- Function of the SPS thresholds in the front and rear walls
- Function of the lepton-scattering angle

Determination of p'_{min} (e^-) for MUSE

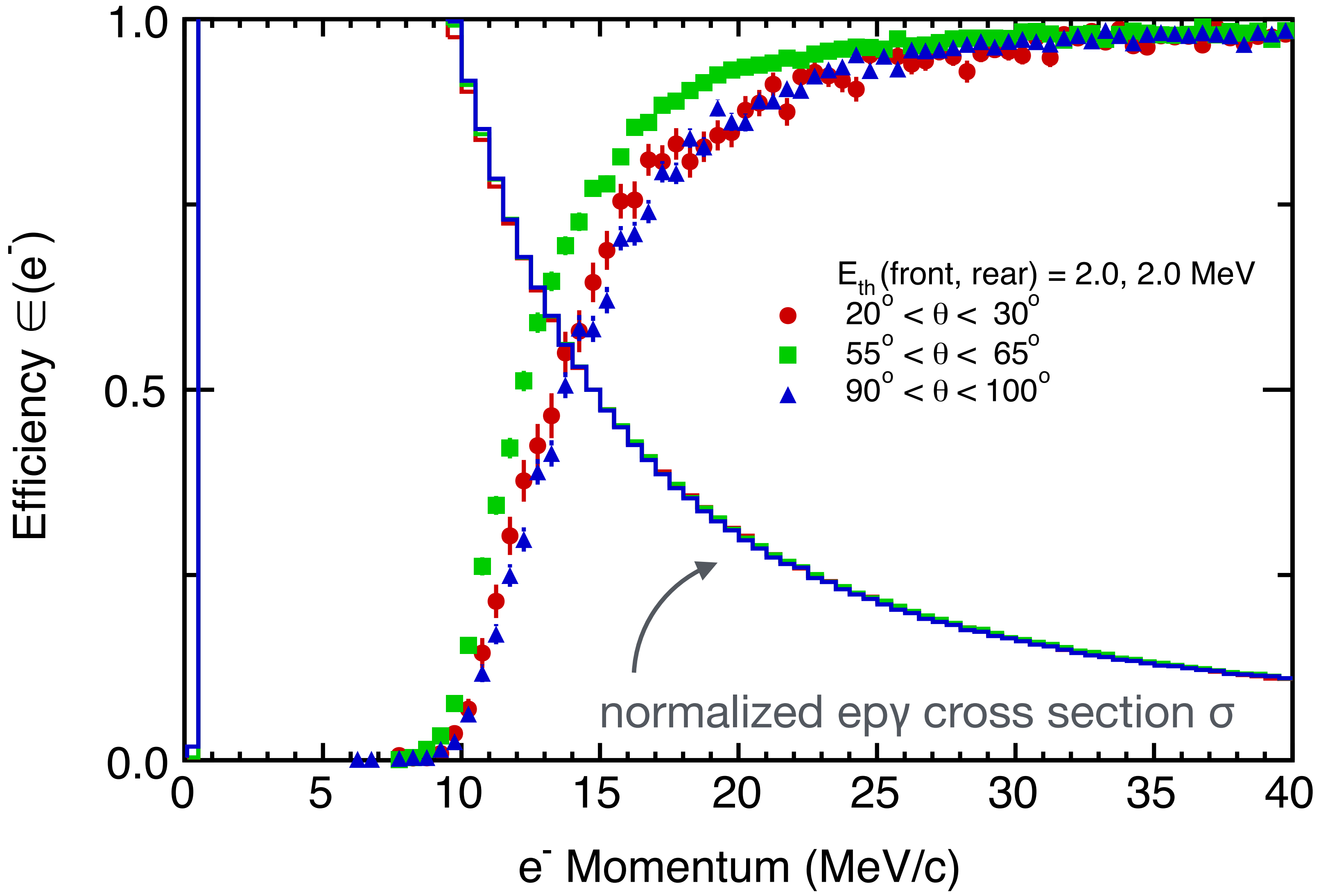

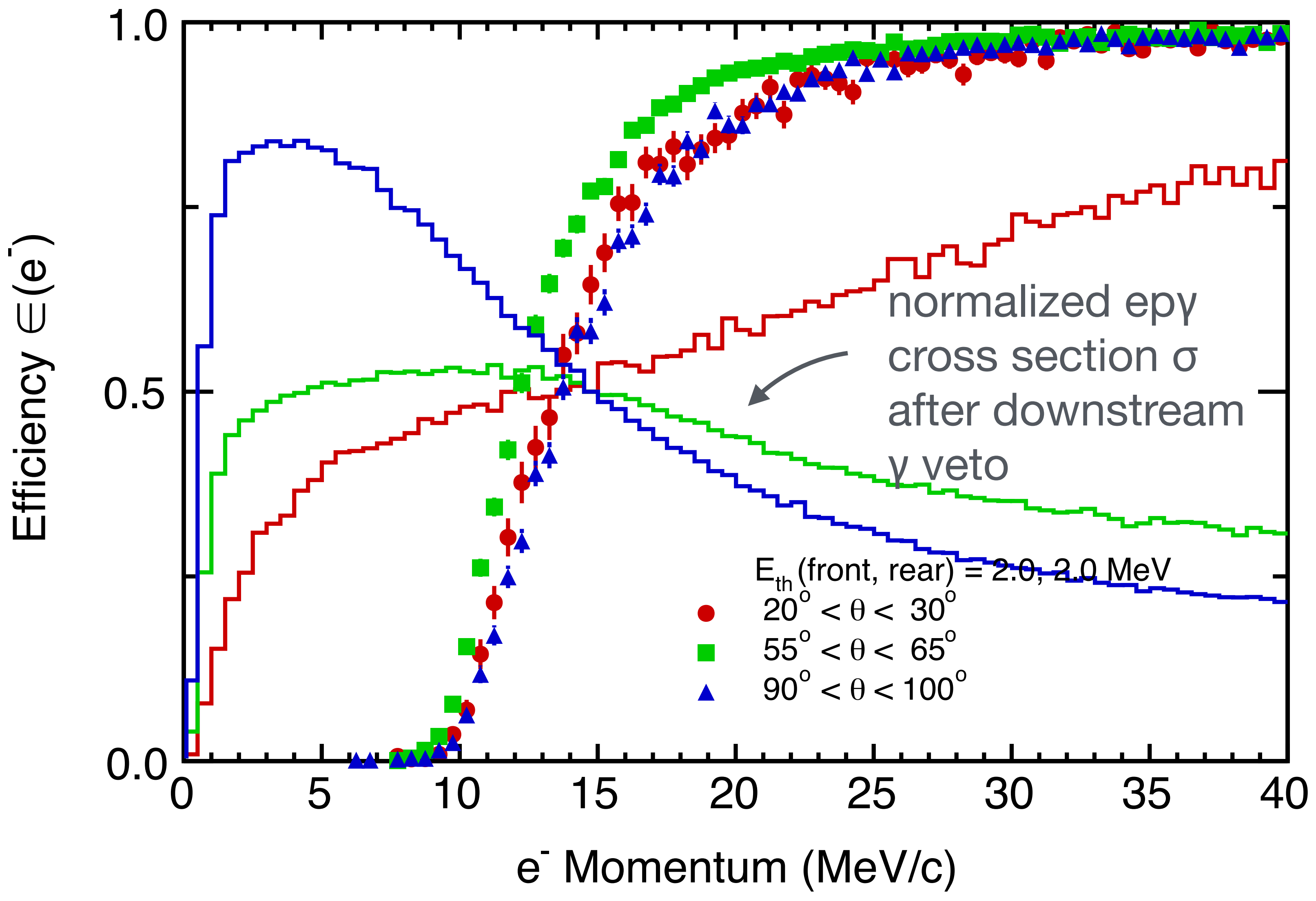

$$\int_0^{p_{max}} \epsilon(p') \frac{d\sigma(p')}{dp'}\, dp' = \int_{p'_{min}}^{p_{max}} \frac{d\sigma(p')}{dp'} dp'$$

p'_{min} (MeV/c)	Weight		
	1	σ	**σ with γ veto**
25°	14.6	14.8	**13.7**
60°	13.2	12.5	**13.0**
95°	14.9	14.0	**14.4**

Effective p'_{min} also

- depends on the cross-section weight,
- is affected by calorimeter analysis.

$\sigma_{p'_{min}} < 2$ MeV/c

Muon detection threshold in the SPS

Muons detected in the SPS detectors

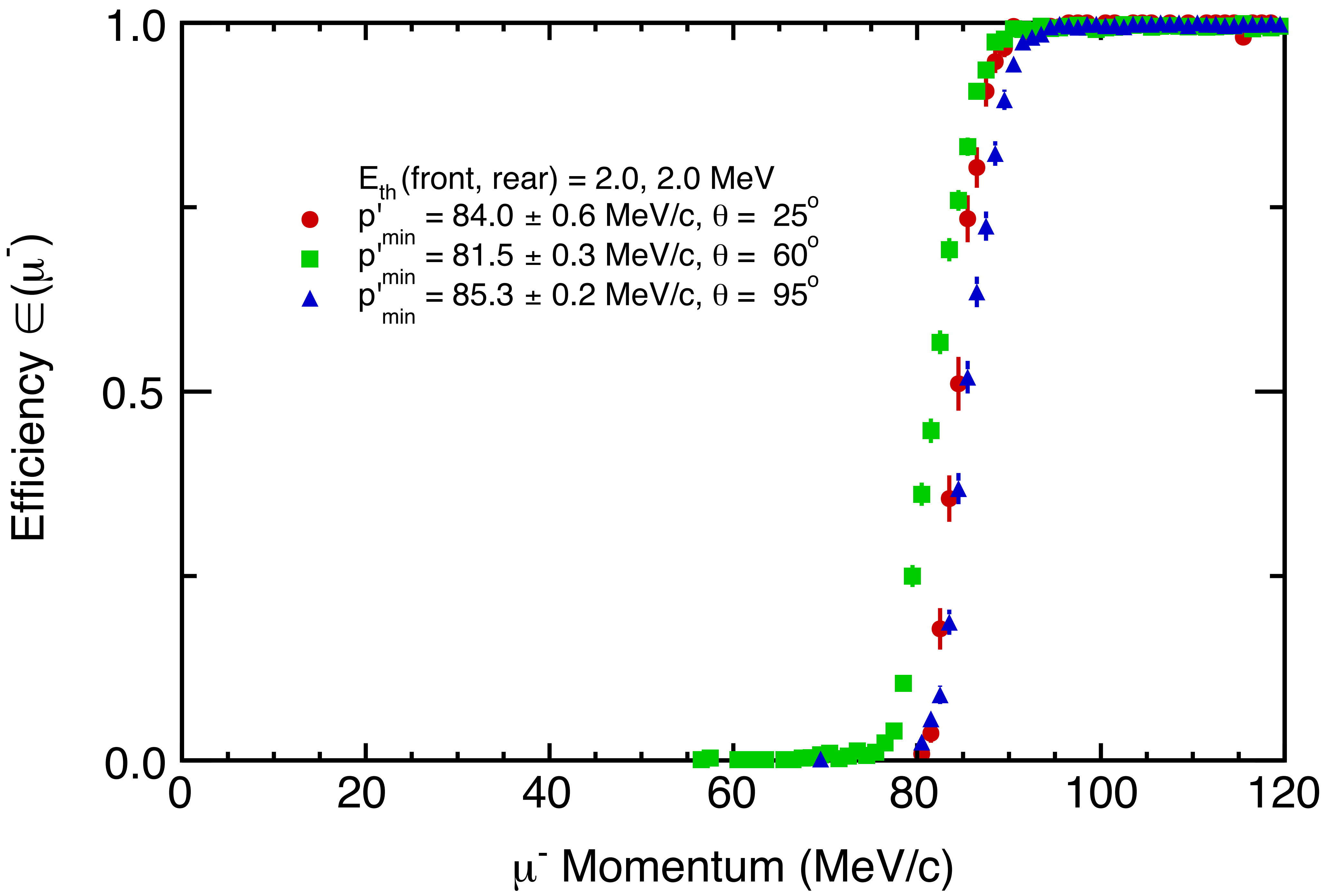

Muons or **secondaries**
detected in the SPS detectors

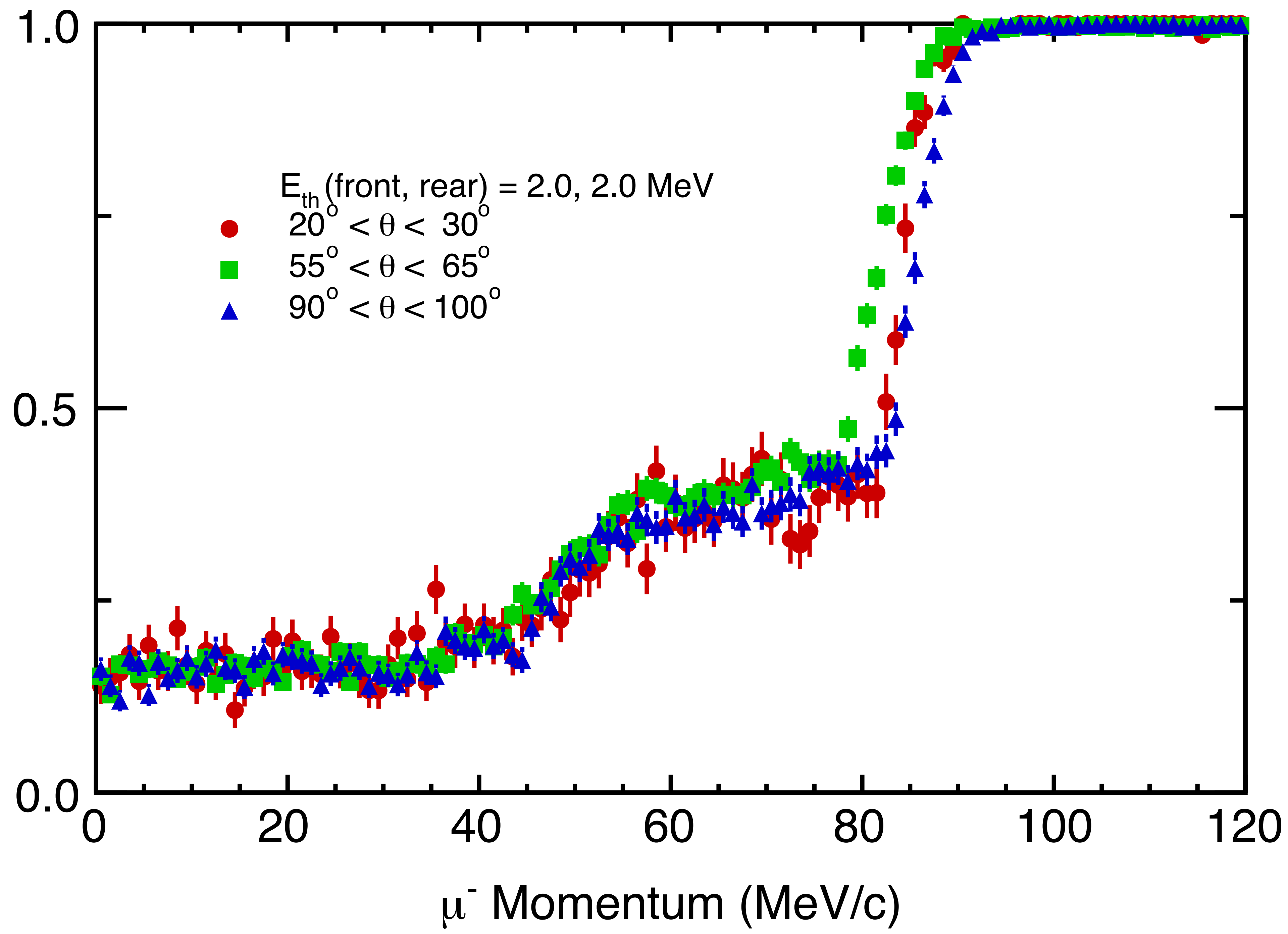

The muon-detection threshold is complicated

The elastic muon-proton cross section is minimal close to threshold threshold

Upgraded photon calorimeter was commissioned in 2022

$$\delta = \delta(p_0, \theta_l, p'_{min}, \Omega_\gamma)$$

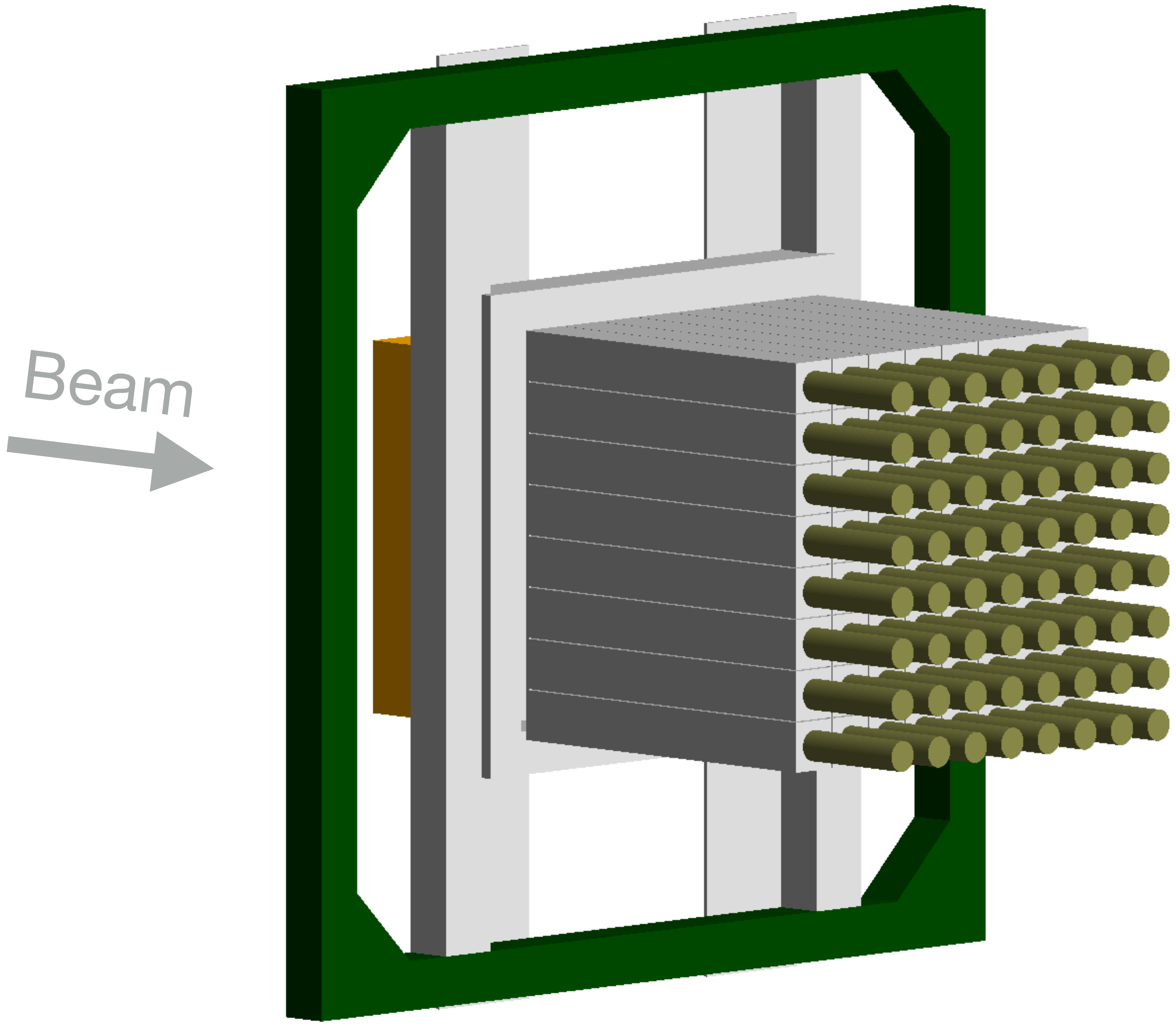

64 lead-glass crystals
(4 cm x 4 cm x 30 cm)

Pulse-height distributions from the 64 channels

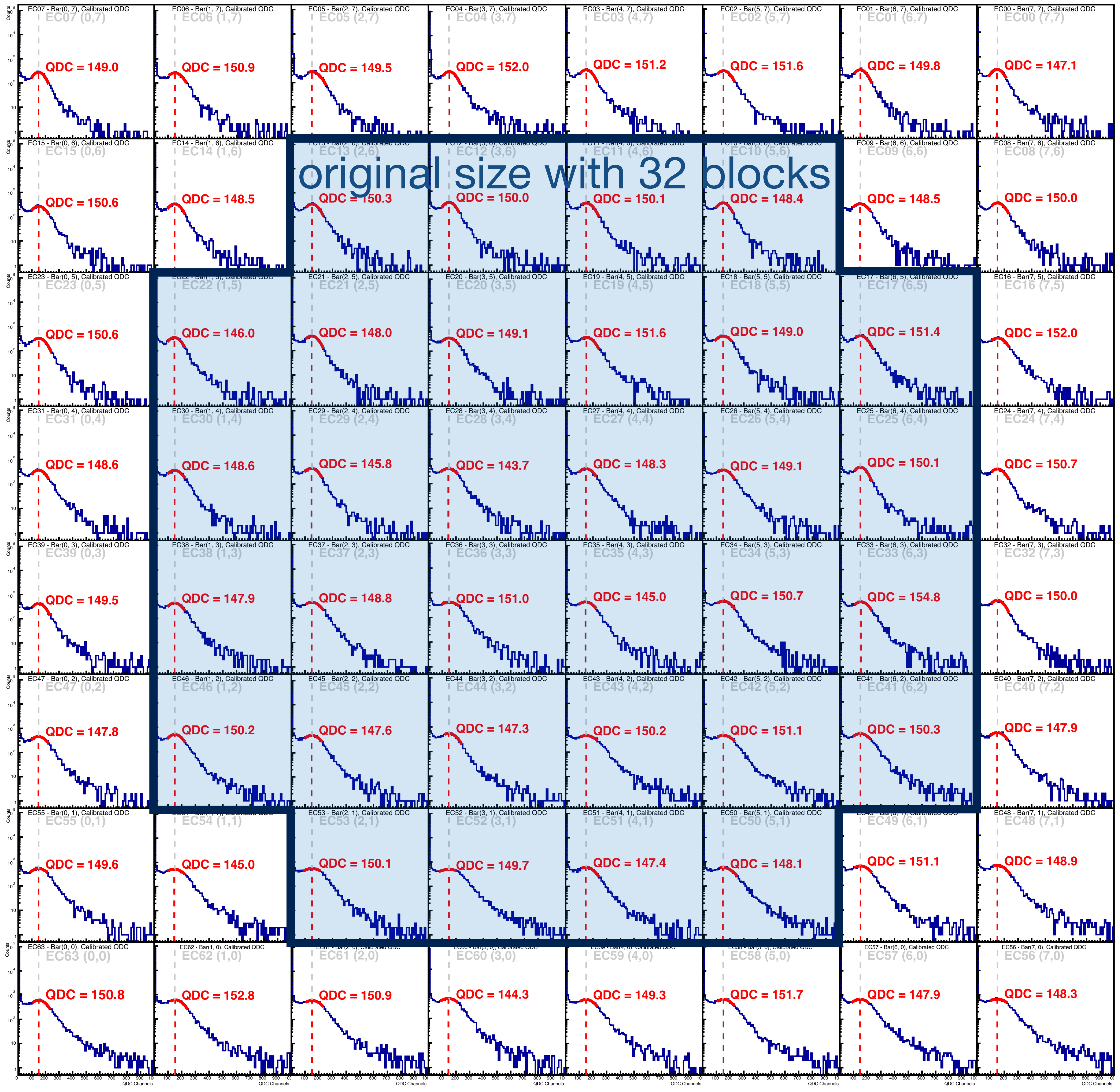

Win Lin's analysis of cosmic-ray events

Calorimeter performance tests

- Momentum scan from 230 MeV/c down to 20 MeV/c
- Electron PID in BH
- BM hit required to ensure charged-particle signal in CAL
- Light-output signal as output sum of nine CAL blocks

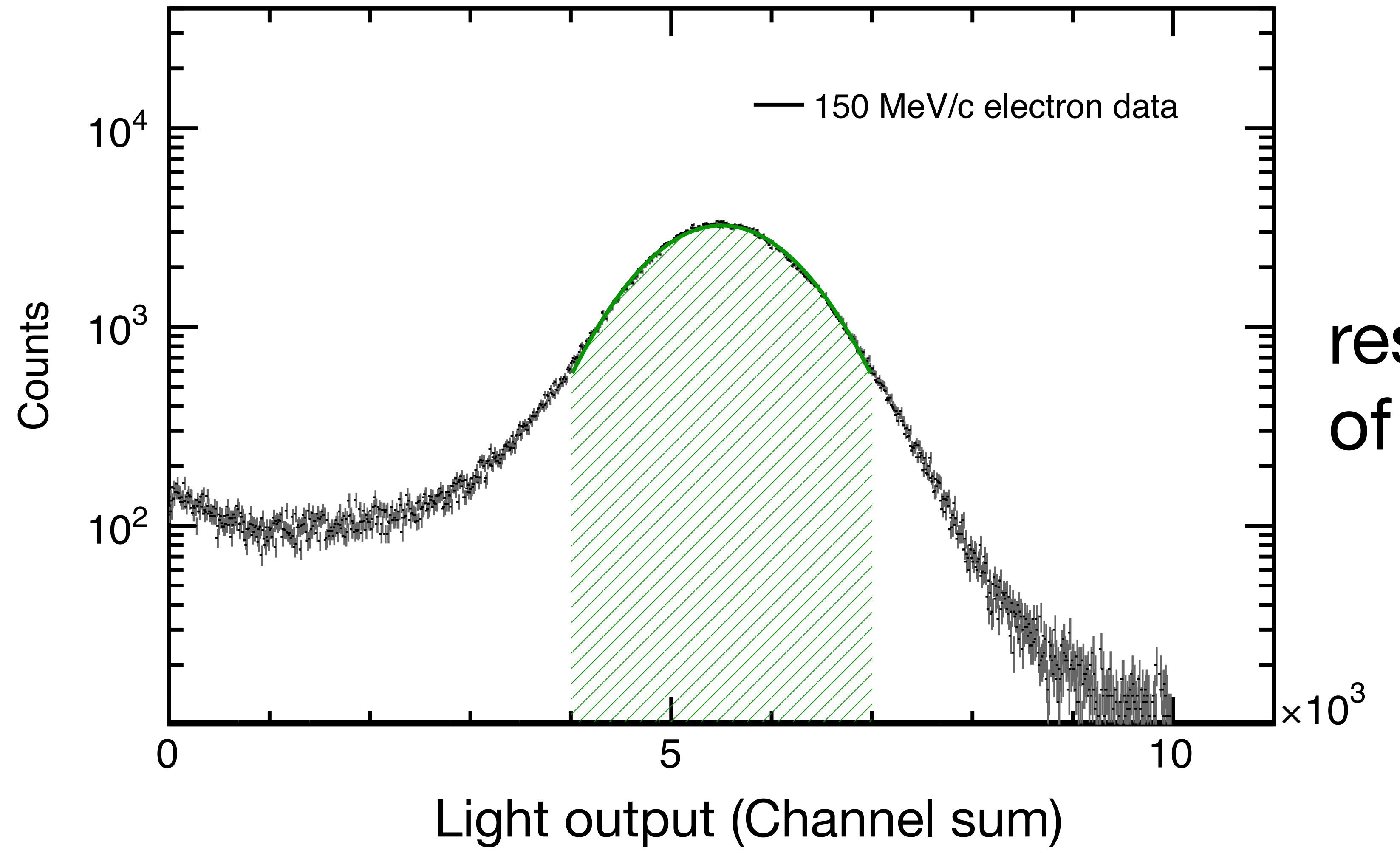

result from one of 22 runs

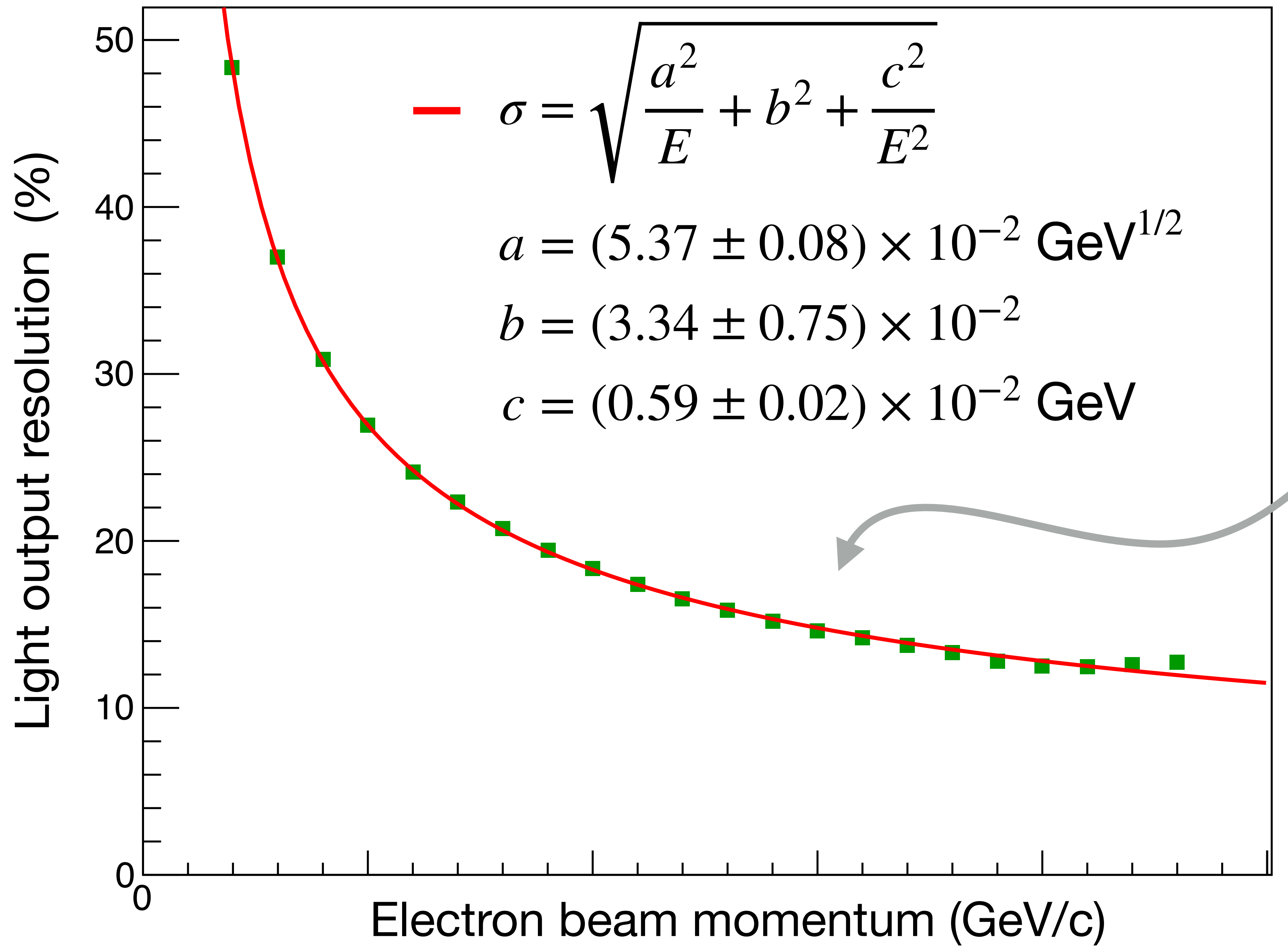

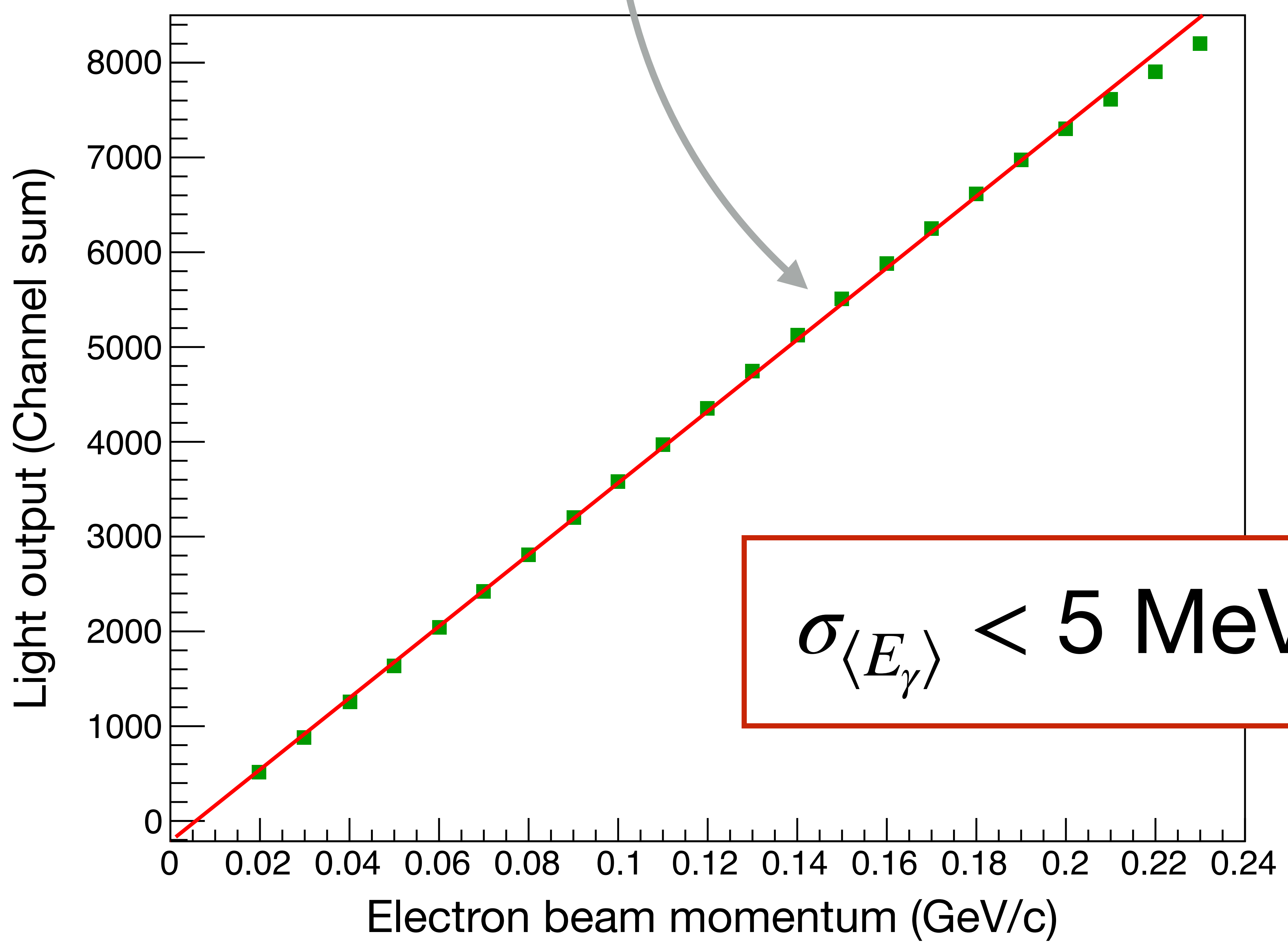

$\sigma_{\langle E_\gamma \rangle} < 5$ MeV

Measurements with the original calorimeter with 32 crystals; Win Lin's analysis

Calorimeter can be used to suppress initial-state bremsstrahlung

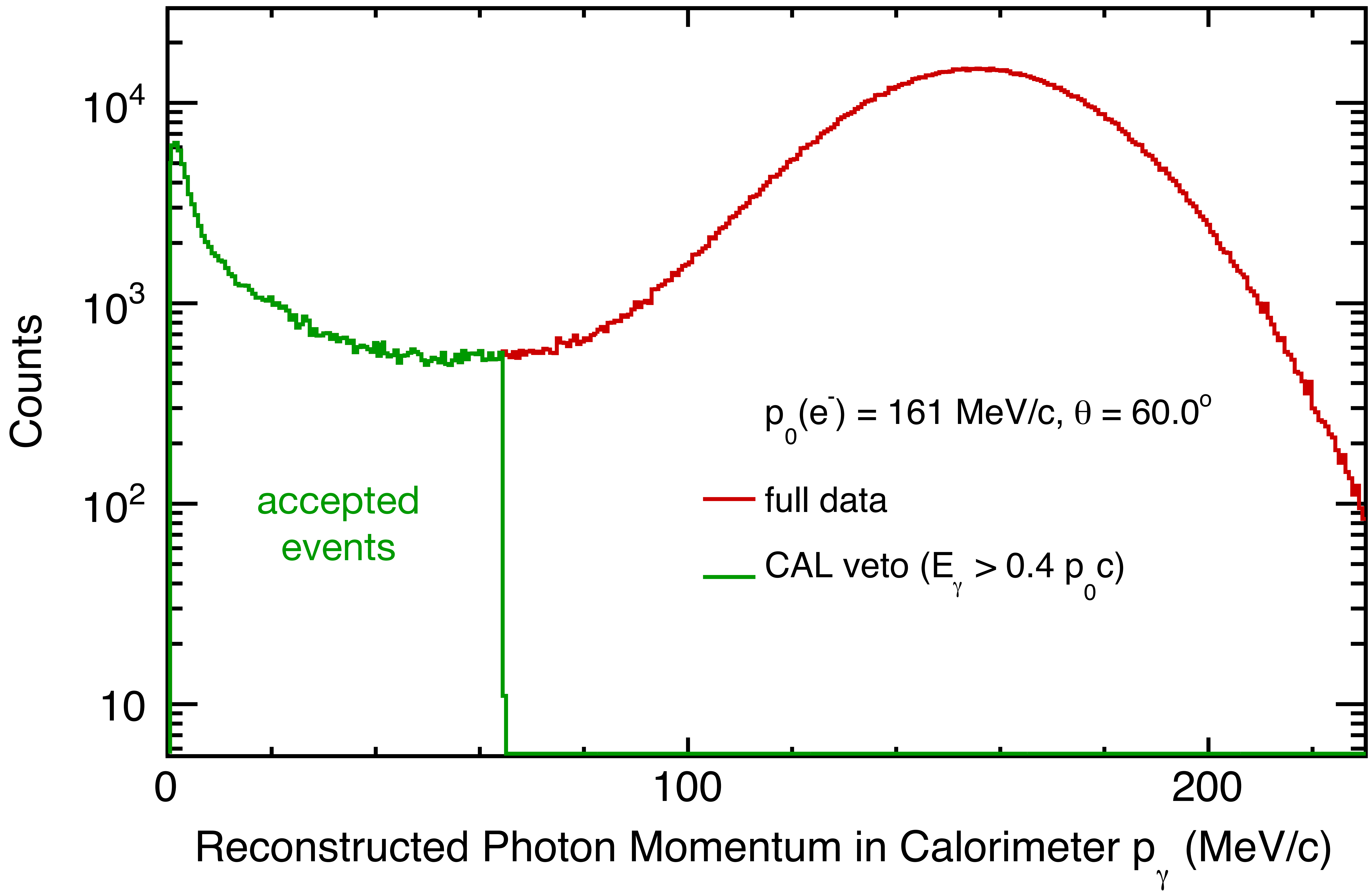

Simulation of measured photon spectrum:

1. ESEPP bremsstrahlung spectrum
2. within the CAL acceptance,
3. folded with the known detector resolution

Simulated downstream $ep \rightarrow e'p\gamma$ photon distribution

p_0 = 161 MeV/c
$\theta_{e'}$ = 60°

full distribution

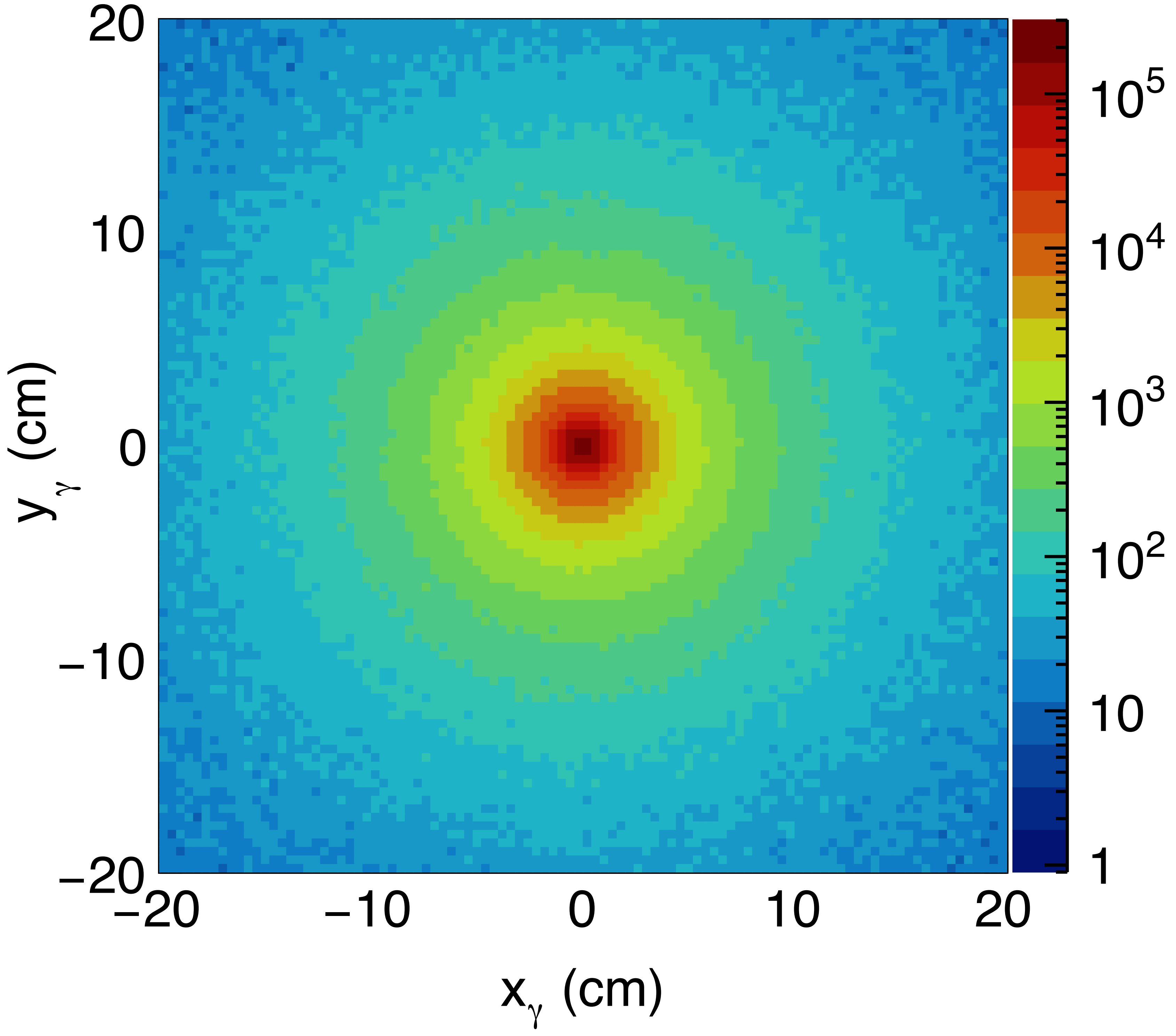

distribution after cut on calorimeter signal

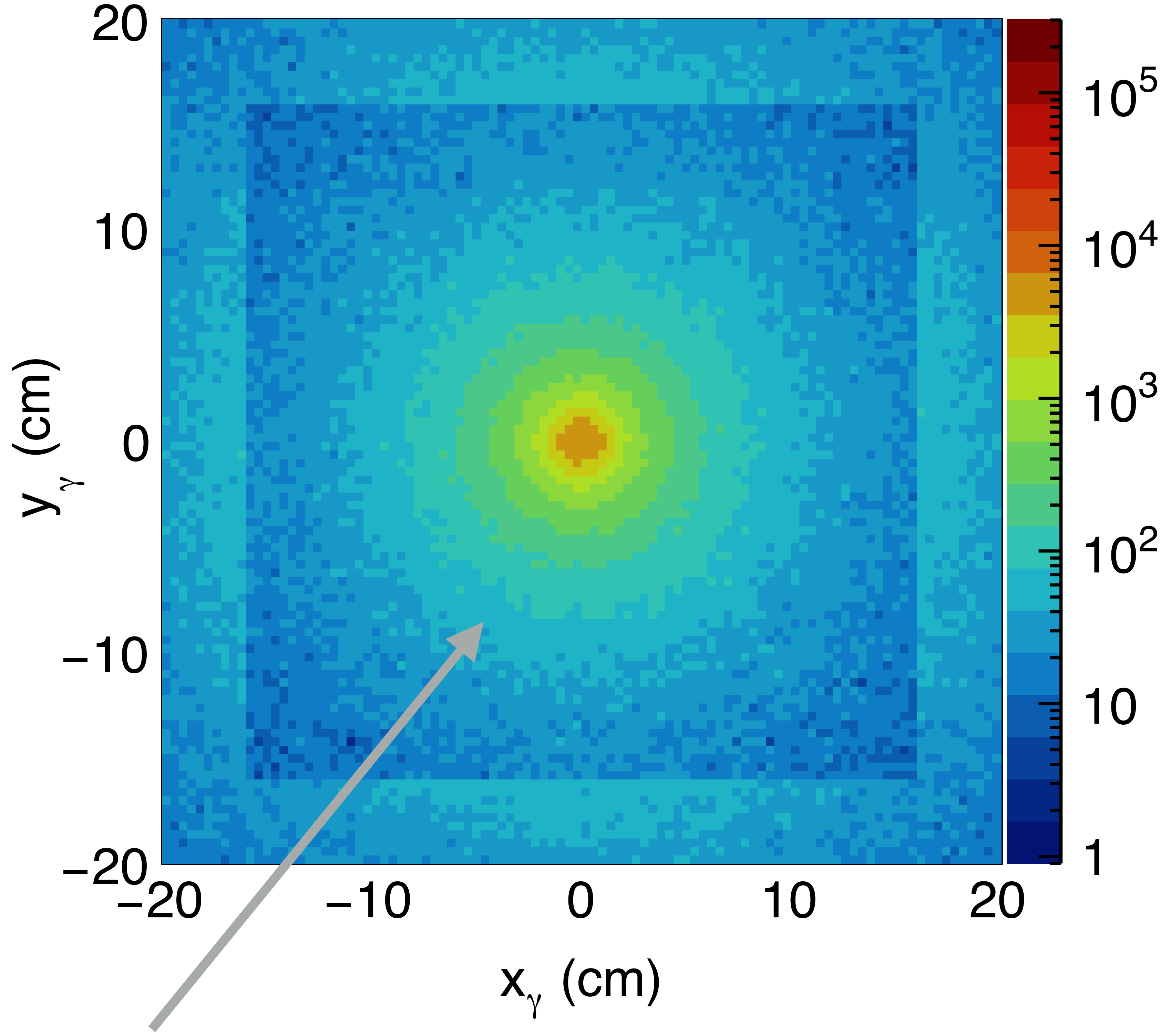

photons with low reconstructed momentum, below selected calorimeter cutoff energy

Radiative corrections for e^-p scattering data in MUSE kinematics

Rapidly changing radiative corrections for small $p'_{min.}$

(> 1% change / MeV/c)

CAL veto on downstream photons reduces radiative corrections and p'_{min} dependence, reducing uncertainty.

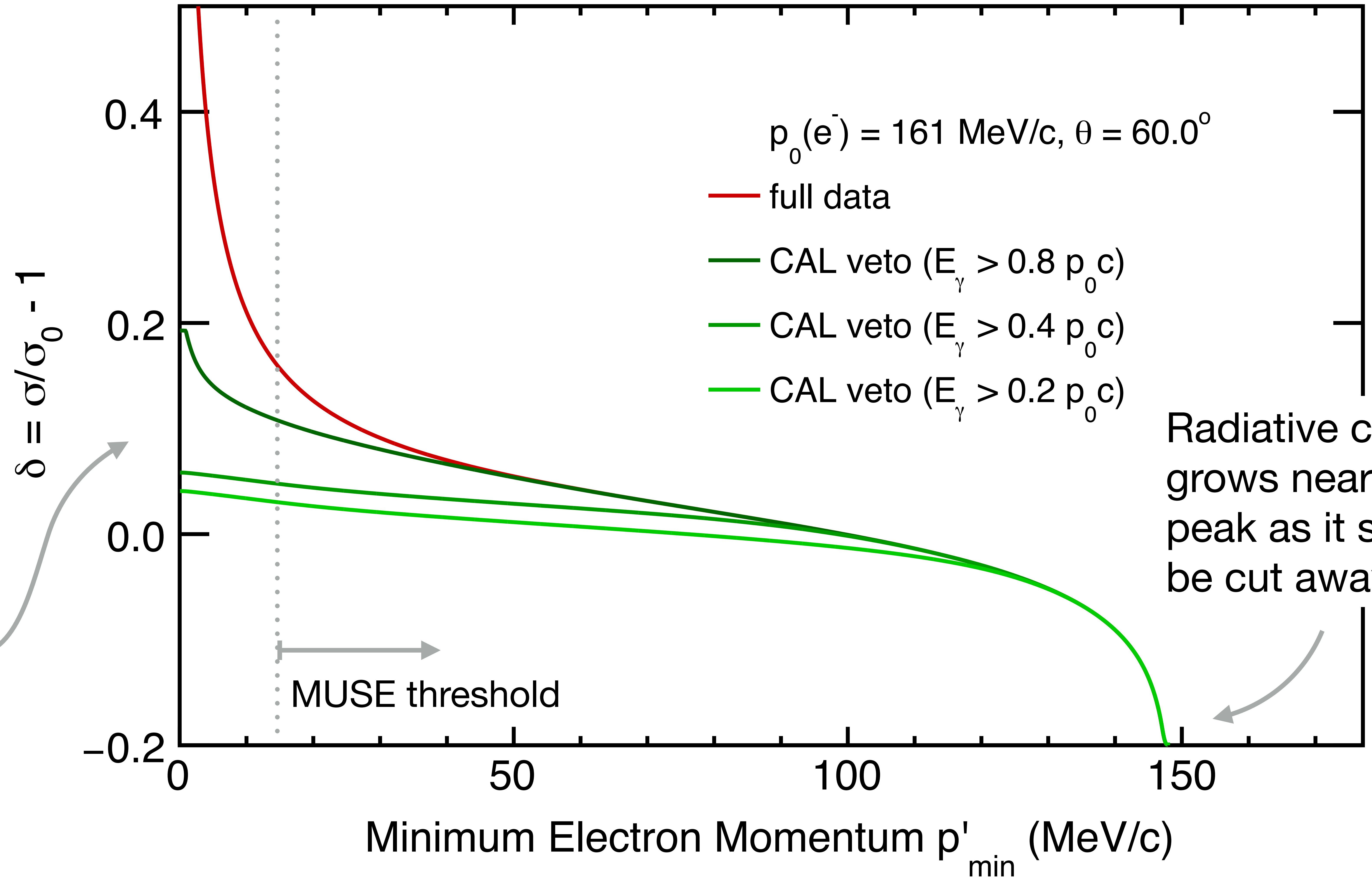

Radiative correction grows near elastic peak as it starts to be cut away.

Minimizing the overall uncertainty with optimal photon-energy cut

$$\sigma^2(\delta) = \left(\frac{\partial \delta}{\partial p'_{min}}\right)^2 \sigma^2(p'_{min}) + \left(\frac{\partial \delta}{\partial E_\gamma^{cut}}\right)^2 \sigma^2(E_\gamma^{cut})$$

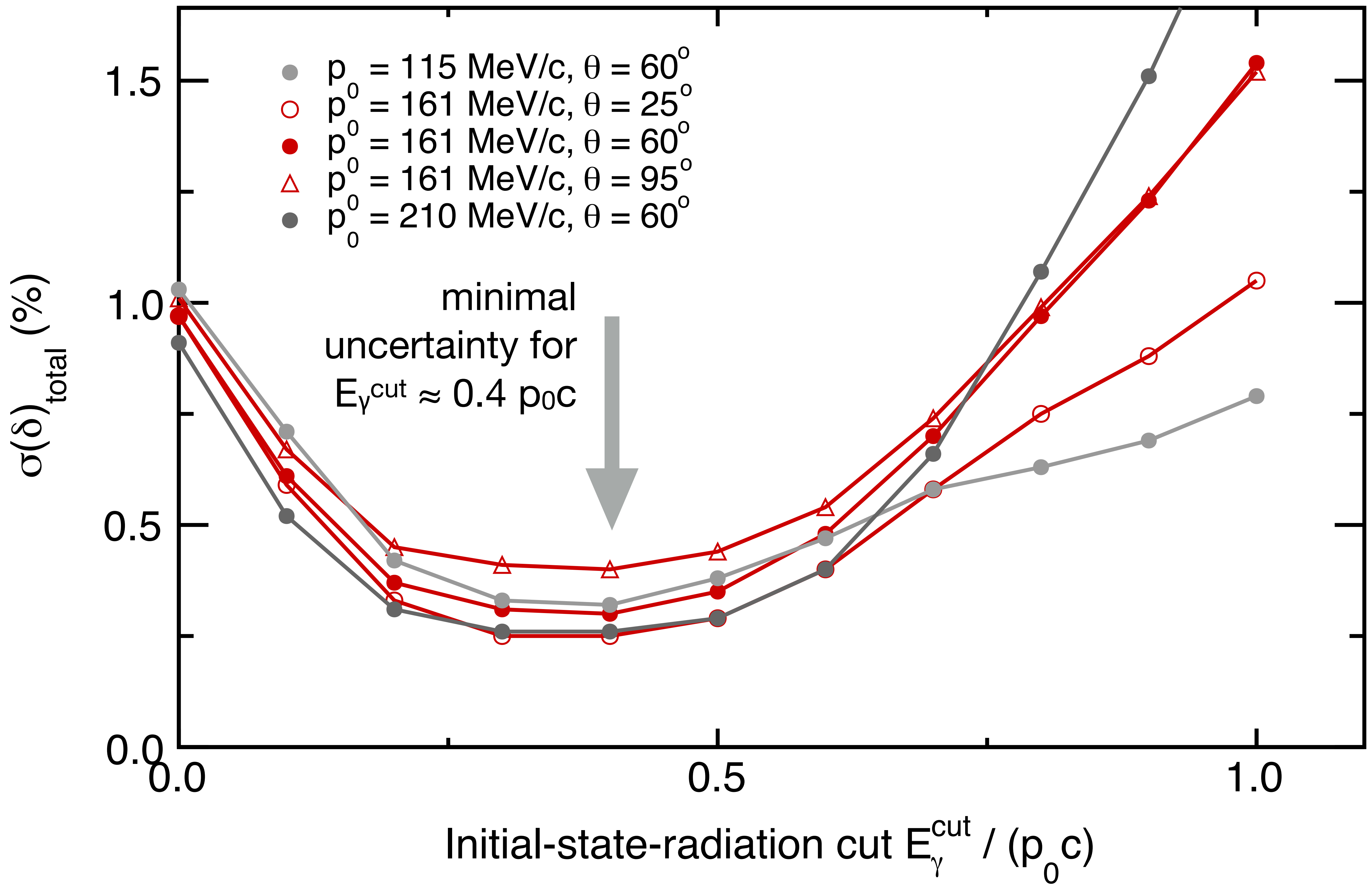

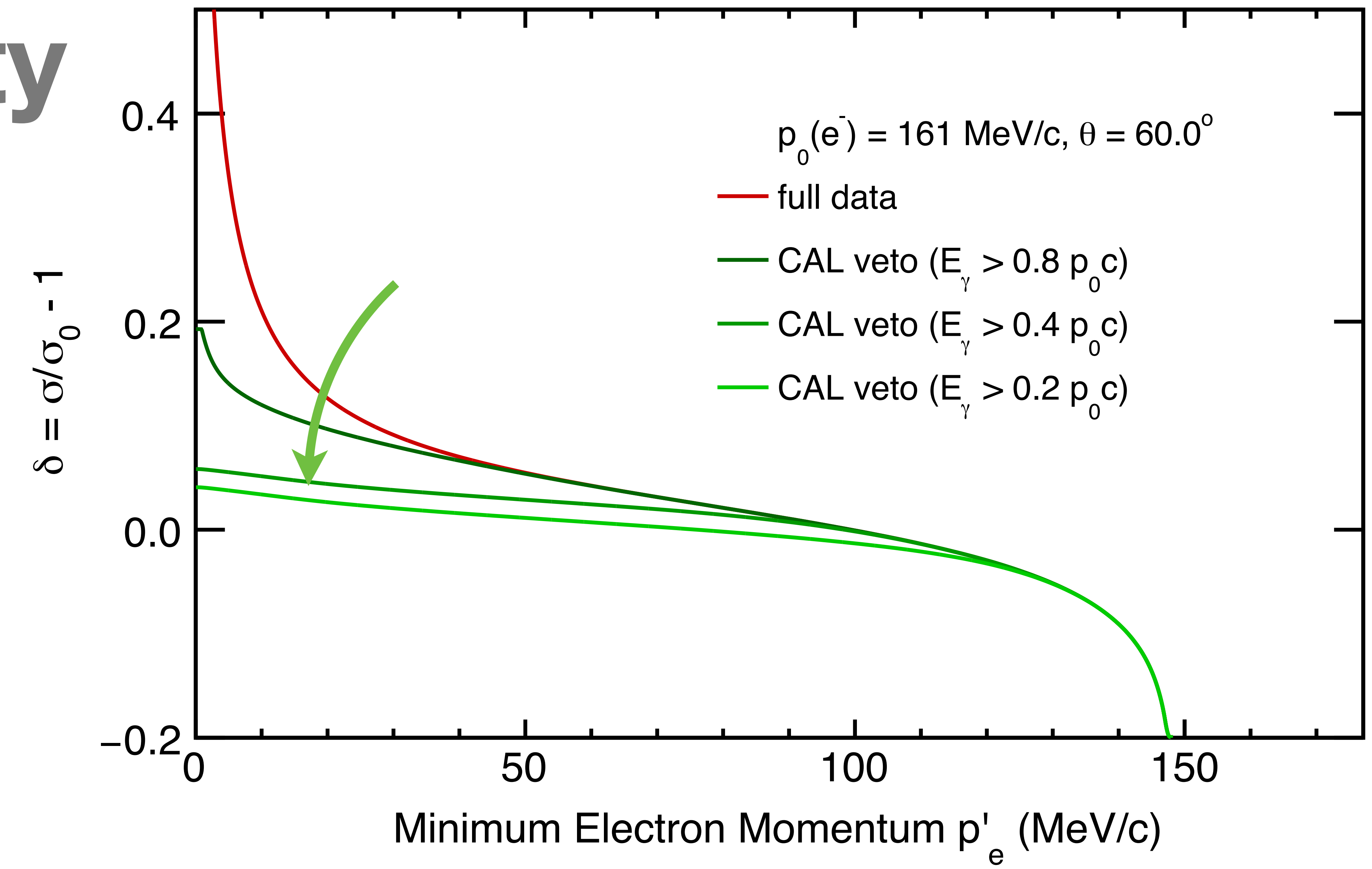

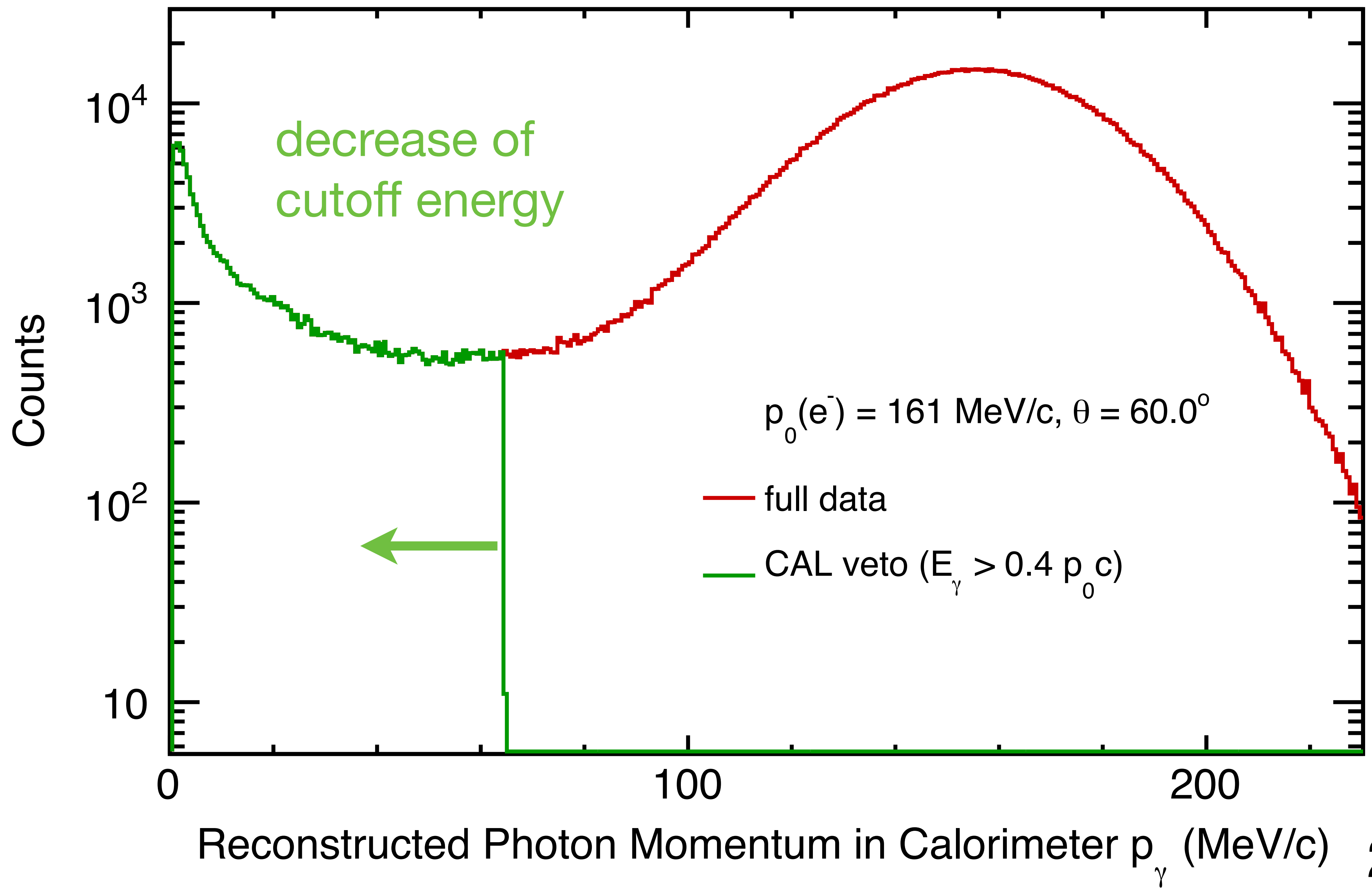

Radiative corrections for $\mu^- p$ scattering data in MUSE kinematics

Radiative corrections are less than 1%

Corrections are nearly independent of p'_{min}

Calorimeter cut is without effect on the data

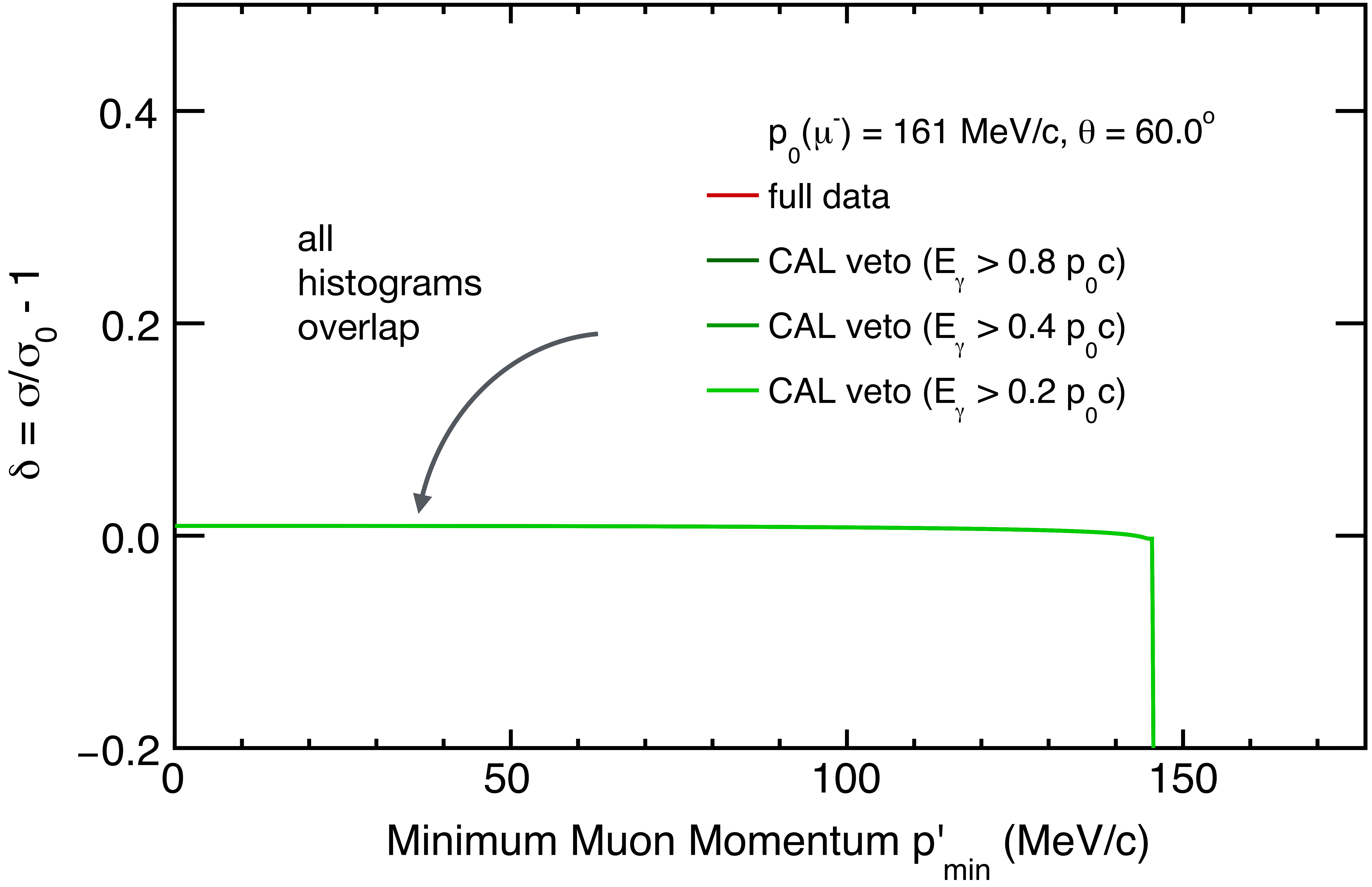

Uncertainties in the radiative corrections

- The preliminary estimates of the total uncertainties in the radiative corrections for **electrons** are 0.2% - 0.5%.*

$\sigma_\delta(e^-)$	115 MeV/c			161 MeV/c			210 MeV/c		
	20°	60°	100°	20°	60°	100°	20°	60°	100°
p'_{min}	0.05%	0.18%	0.30%	0.03%	0.16%	0.31%	0.02%	0.13%	0.31%
θ	0.01%	0.01%	0.00%	0.01%	0.00%	0.00%	0.00%	0.03%	0.01%
p_0	0.00%	0.00%	0.00%	0.00%	0.00%	0.00%	0.00%	0.00%	0.00%
E_γ	0.32%	0.33%	0.33%	0.25%	0.25%	0.26%	0.20%	0.22%	0.22%
Total	**0.32%**	**0.38%**	**0.45%**	**0.25%**	**0.30%**	**0.40%**	**0.20%**	**0.26%**	**0.38%**

angle-dependent uncertainty, relevant for radius extraction, $\lesssim$ 0.3%

angle-**in**dependent uncertainty, **not** relevant for radius extraction

- The preliminary estimates of the total uncertainties in the radiative corrections for **muons** are smaller than 0.01%.*

* Not including model uncertainties.

Cross-section asymmetries (differential)

The interference-TPE term and the interference-bremsstrahlung terms change sign depending on the sign of the lepton's charge.

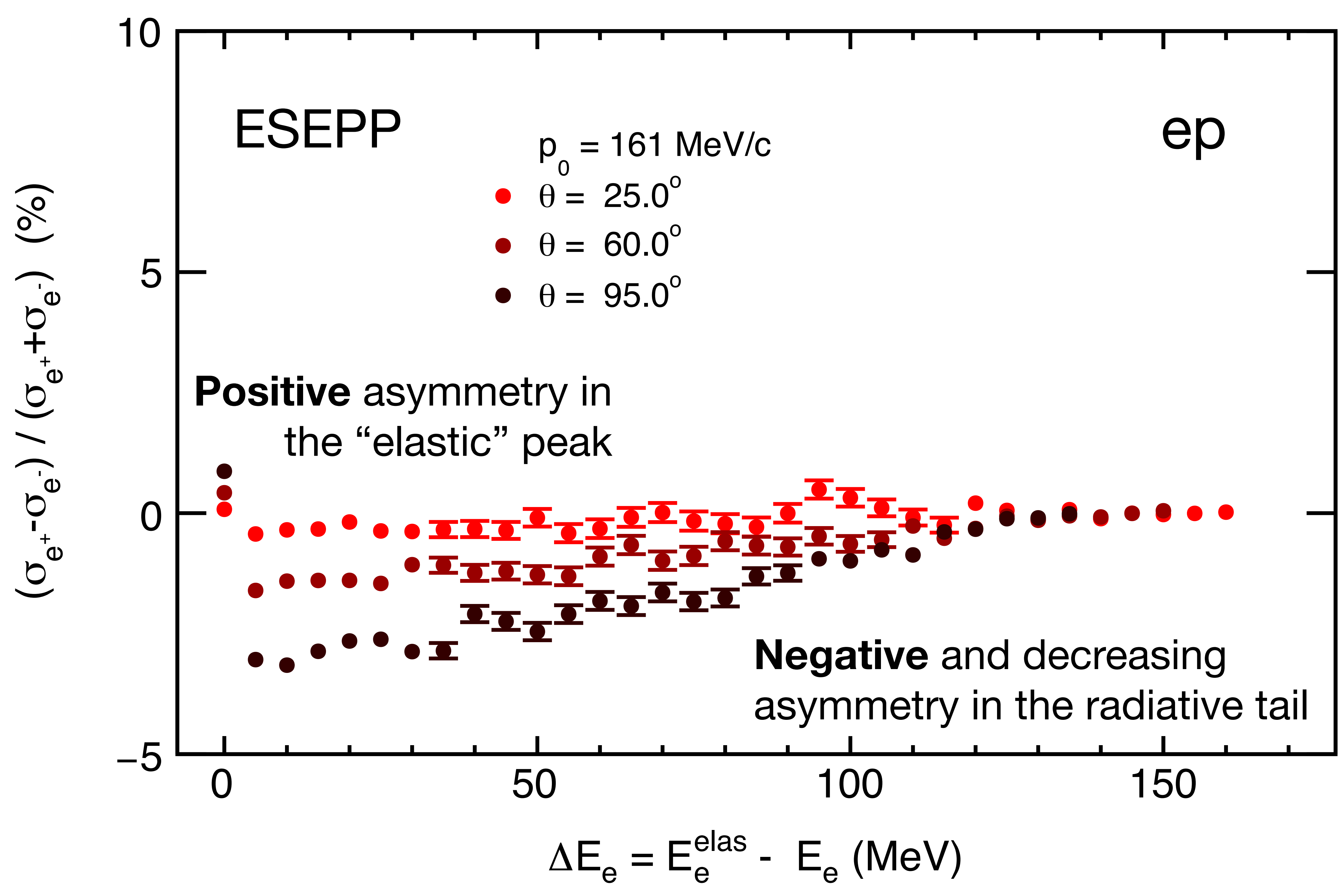

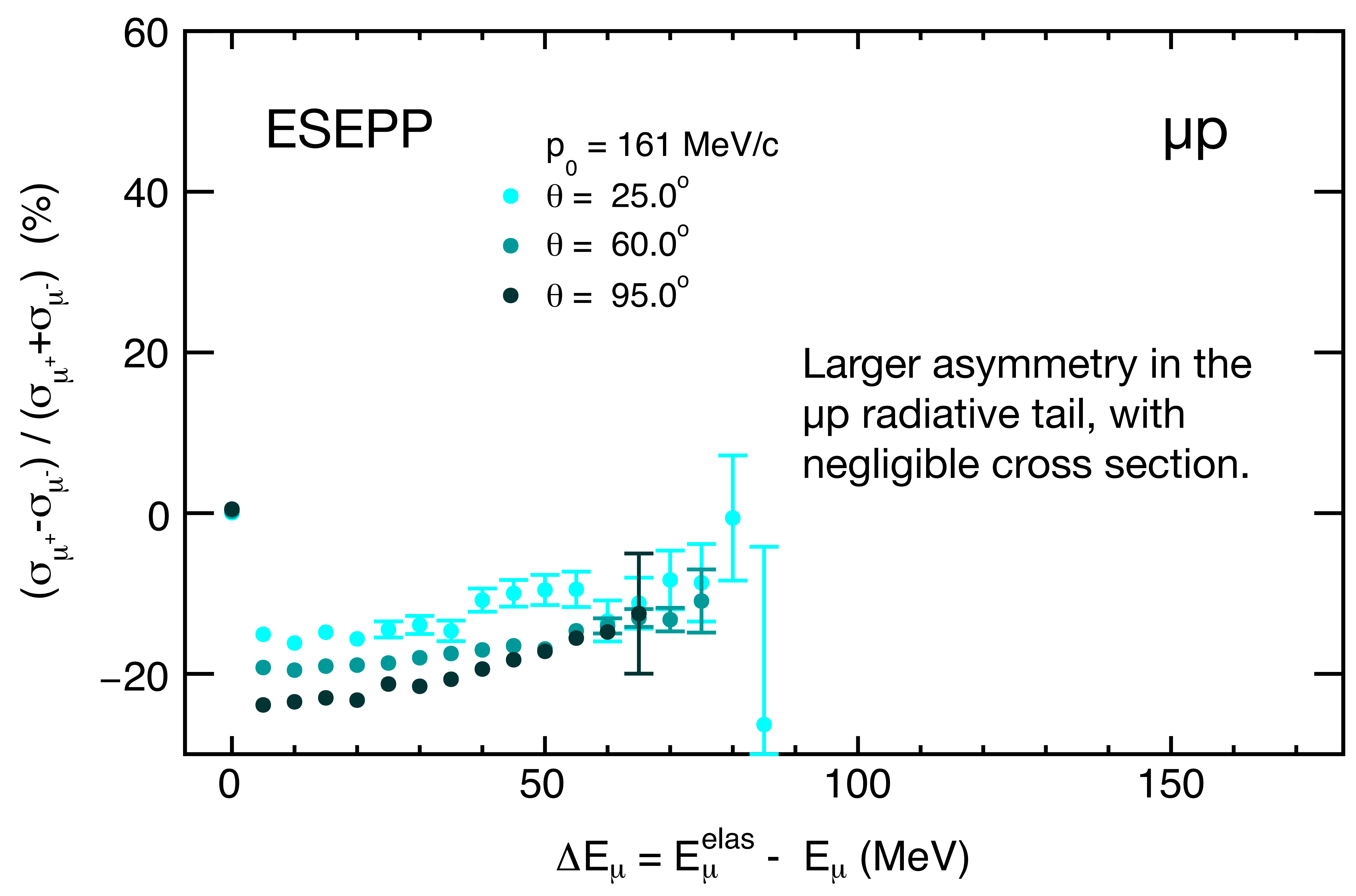

Cross-section asymmetries (integrated)

Asymmetries of the integrated cross sections

$$\frac{d\sigma}{d\Omega} = \int_{p'_{min}} \frac{d^2\sigma(p')}{dp'd\Omega}\, dp'$$

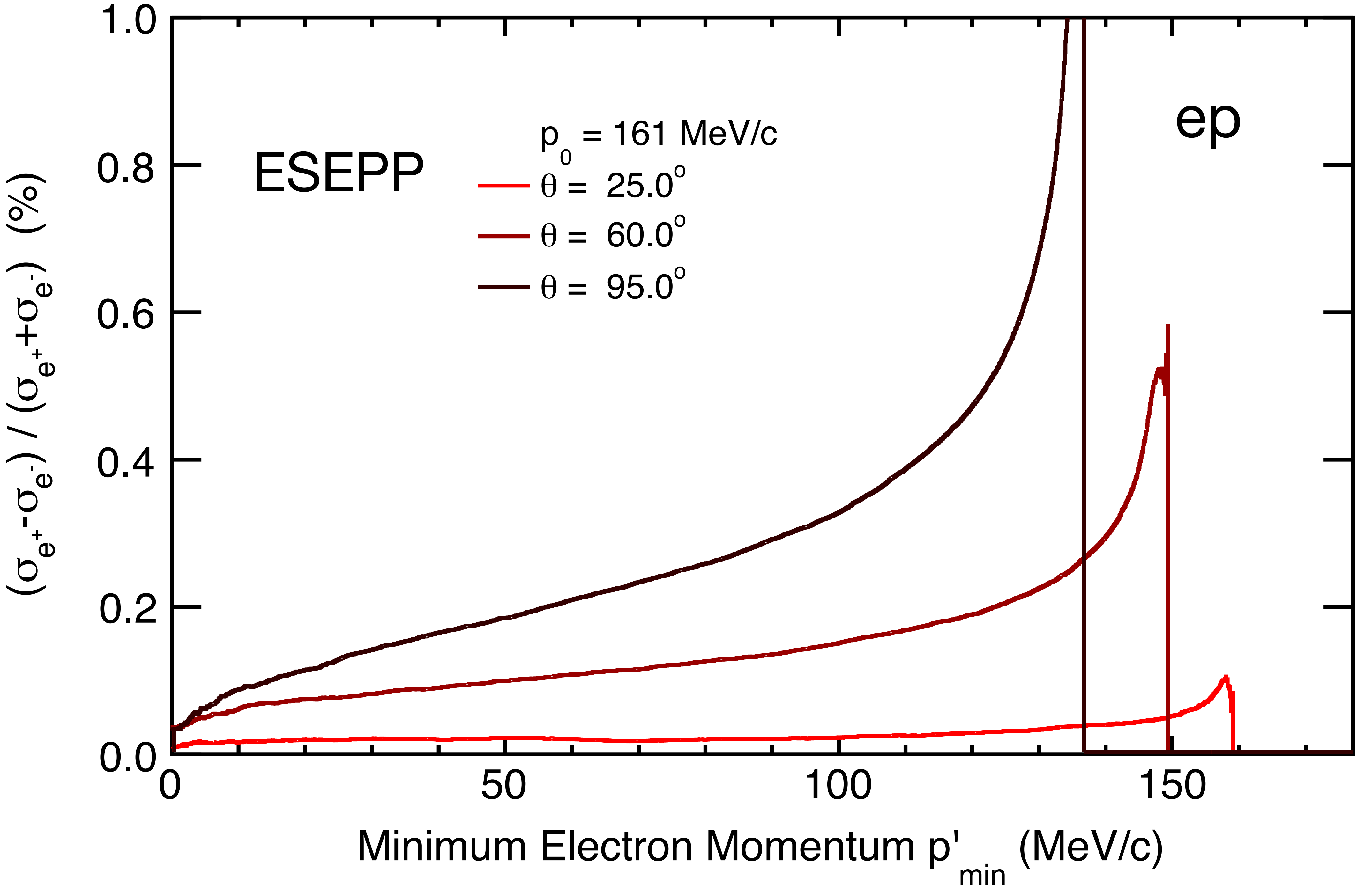

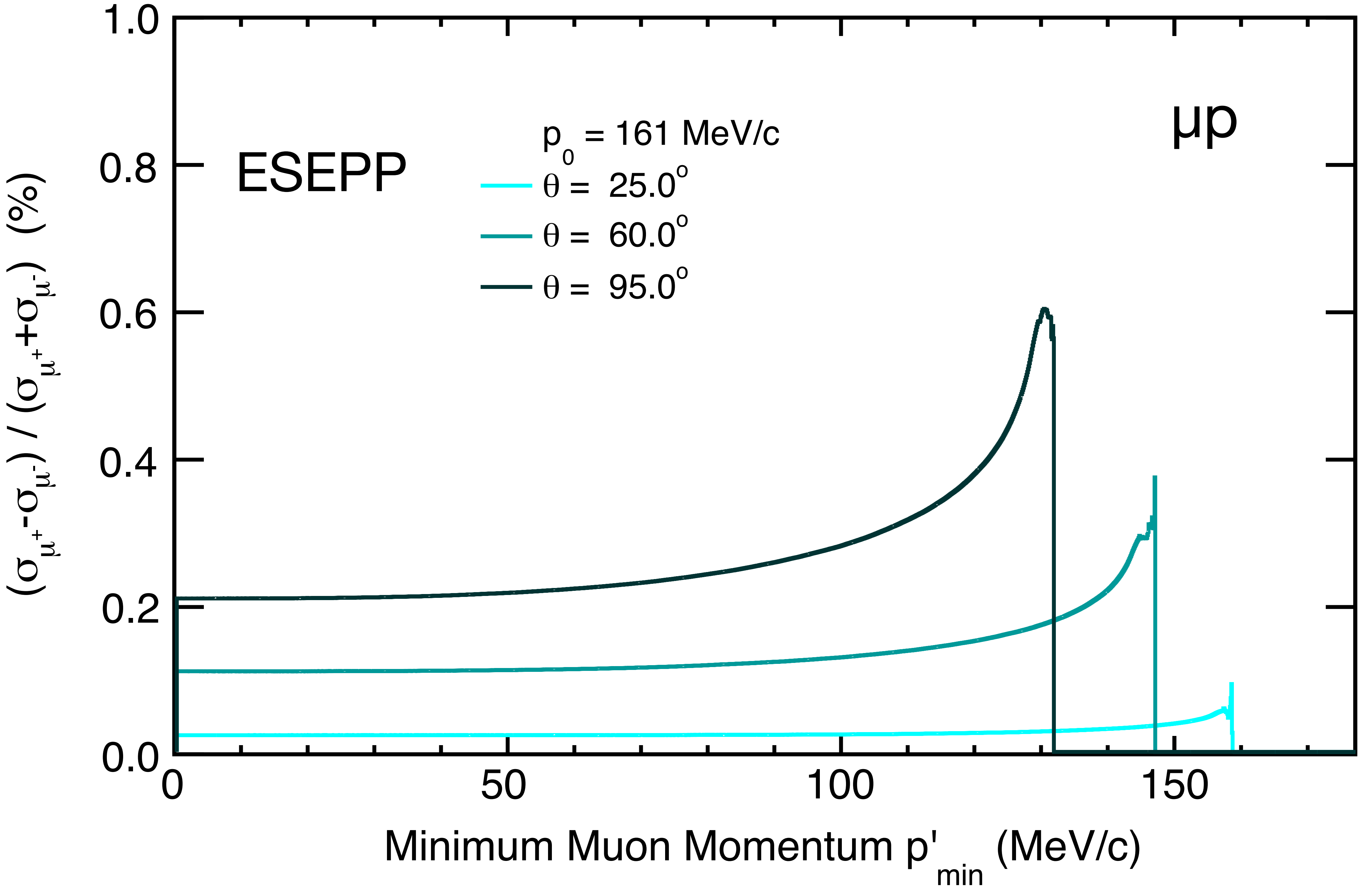

- Decreasing asymmetry with decreasing p'_{min}
- Decreasing asymmetry with decreasing Q^2
- Higher asymmetry for the lighter lepton (close to the elastic peak)

The low values of p'_{min} will result in small cross-section asymmetries for MUSE

See also: A. Afanasev and A. Ilyichev, Phys. Rev. D 105, L011301 (2022)

Summary

- **The MUSE setup** has unique implications for the determination of radiative corrections:
  - Without a magnetic spectrometer, MUSE integrates over a range of final-state lepton momenta.
  - A dedicated downstream photon detector helps to suppress initial-state radiation effects.
- ESEPP simulations show angular-dependent uncertainties in radiative corrections to the electron cross section be up to 0.3%.
- Most critical for determination of accurate corrections are:
  - Understanding of the SPS detection threshold and CAL response
  - Validity of the theoretical model